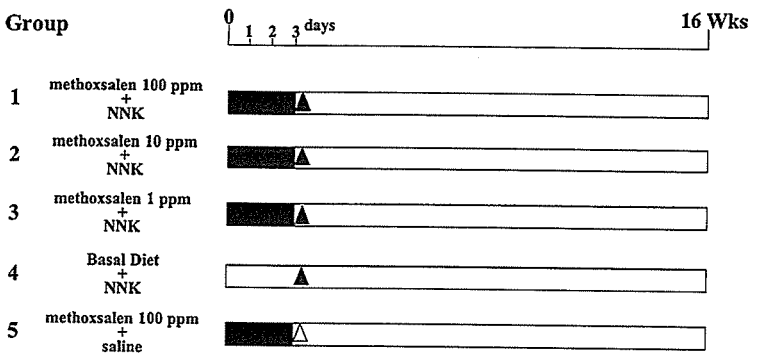

Fig. 1. Experimental design. Animals: A/J female mice, 7 weeks age ■; 8-MOP (100, 10, 1 ppm, p.o.), □: basal diet (vehicle control; Labo. MR, p.o.), ▲: NNK (2 mg/mouse, i.p.), △: saline (vehicle control; 0.1 ml/mouse, i.p.).

stereomicroscope, and each lung lobe was examined histopathologically.

2.4. Subjects for mRNA quantitation

In a separate experiment, mice at 7 weeks of age were treated with 8-MOP (50, 5 or 0.5 mg/kg body weight in 0.2 ml corn oil, given by stomach tube) or an equal volume of corn oil (vehicle control) daily for 3 days. All mice were killed at one hour following final 8-MOP treatment for lung and liver RNA isolation and quantitative analysis of CYP2As.

2.5. RNA isolation

Total RNA was isolated from 30 mg aliquots of whole lung and liver tissues using RNAlater RNA Stabilization Reagent (Qiagen Corp., Hilden, Germany) and an RNeasy Mini Kit (Qiagen Corp., Hilden, Germany). The concentration of RNA was measured from the absorbance at 260 nm and first strand cDNA was synthesized from 400 ng of total RNA using TaqMan Reverse Transcription Reagents (Applied Biosystems, Foster city, CA) according to the manufacturer's instructions.

2.6. Quantitative real-time RT-PCR

Optimal primers and probes were selected using Software Primer Express Ver.1.7 (Applied Biosystems, Foster city, CA). The TaqMan Rodent glyceraldehyde-3-phosphate dehydrogenase (GAPDH) Control Reagent (Applied Biosystems, Foster City, CA) was used for PCR of GAPDH mRNA as an internal control. The sequences of primers and TaqMan probes for mouse CYP2A4 and CYP2A5 mRNAs were as follows: CYP2A4, forward 5′-GCTATGGCTTTCTGTTGCTCATG-3′, reverse 5′-ATCACCCGATCAATCTCCTCAT-3′, and probe, 5′-TTGAGGCCAAGGTC-3′; mouse CYP2A5, forward 5′-CCAACGTTATGGTCCTGTATTCAC-3′, reverse 5′-TCCACCAGAGCTTCCTTGACT-3′, and probe 5′-ACAGCACCACAATTC-3′. The sequences of primers and TaqMan probes for GAPDH mRNA were no known because of purchasing from Assays-on-demand system of ABI (Applied Biosystems, Foster city, CA).

Quantitative real-time RT-PCR was performed in an ABI PRISM 7000 Sequence Detection System using specific primers and TaqMan probes for mouse CYP2A4 and CYP2A5. PCR was carried out in 50 uL reaction mixtures containing 25 uL of 2×TaqMan Universal PCR Master Mix, 50 ng of cDNA, 100 nM of each primer, and 200 nM of TaqMan probe. Cycling conditions were as follows: 2 min at 50 °C, 10 min at 95 °C, and then 40 cycles of 15 s at 95 °C followed by 1 min at 60 °C. PCR amplification of GAPDH mRNA was similarly carried out. TaqMan PCR products were detected as an increase in fluorescence from cycle to cycle. The amplification plots of the PCR reaction were used to determine the threshold cycle (Ct). The Ct value represented the PCR cycle at which an increase in reporter fluorescence (ΔRn) above the line of the optimal value was

first detected. The initial copy number of the target mRNA was calculated by a plot of the Ct against the input target quantity.

Both the precise amount and quality of total RNA are difficult to assess. Therefore, we also quantified transcripts of GAPDH gene as an internal control according to quantitative RT-PCR. Normalization of the data was achieved by quantitating the cycle number at an arbitrary fluorescence intensity in the linear exponential phase and calculating the ratio of the cycle number of each enzyme relative to that of GAPDH.

2.7. Statistical analysis

The data for final body weights were analyzed by the Student's *t*-test. The incidences of lung proliferative lesions were analysed by the Fisher's exact probability test and data for multiplicity by the Student's *t*-test. Dose dependence of the inhibitory effects of 8-MOP was assessed with the Spearman's rank correlation coefficient. Mouse CYP2A4 and CYP2A5 mRNA levels were analyzed by the Kruskal–Wallis test.

3. Results

The results for final body weights and intake of 8-MOP in A/J mice fed diets containing 8-MOP are shown in Table 1. Final body weights did not significantly differ among the groups. The average of daily 8-MOP intake in groups 1–5 was 21.39, 2.45, 0.24, 0 and 23.95 mg/kg b.w./day, respectively, increasing in proportion with the compound in the diet. Lung whitish nodules were detected in all groups macroscopically, but were very rare in the 8-MOP 100 ppm+NNK group. Lung proliferative lesions were hyperplasias and adenomas, diagnosed according to the criteria of 'International Classification of Rodent Tumors: The Mouse [18]', and their numbers were counted under a microscope. Lung carcinomas were not found in any of the animals. Incidences and multiplicities of lung proliferative lesions are summarized in Table 2. The values in the 8-MOP 100 ppm-treated Group 1 were significantly lower than in the NNK alone group ($P<0.001$). 8-MOP reduced the multiplicities of NNK-induced lung proliferative lesions in a dose dependent manner (Spearman rank correlation coefficient; $\rho=-0.806$, correction $P<0.0001$).

Data for relative-quantification of CYP2A mRNAs in livers and lungs of A/J mice are summarized in Fig. 2. Expression of mouse CYP2A4 and CYP2A5 mRNAs in liver and lung was not influenced by the 8-MOP treatment.

4. Discussion

The present investigation demonstrated clear inhibitory effects of 8-MOP in the diet on NNK-induction of lung tumorigenesis in female A/J mice. In contrast to our previous study [10], dose dependence was here apparent for multiplicity. Our earlier experiments showed strong inhibition of lung tumorigenesis at 12.5 mg/kg of 8-MOP by gavage. Daily 8-MOP intake in Group 1 fed the diet containing 100 ppm of 8-MOP was calculated to be 21.39±3.16 mg/kg/day, but it is supposed that plasma 8-MOP concentrations achieved were low compared to that with 12.5 mg/kg 8-MOP by gavage. The results suggest that administration of a diet supplemented with CYP2A6 inhibitors have practical potential for chemoprevention of tobacco related lung cancer.

In 16 week bioassays of NNK-induced lung tumorigenesis in A/J mice, multiplicities of lung

Table 1
Final body weights and intake of methoxsalen in A/J mice fed diets containing 8-MOP

Group	Treatment	No.[a]	Final body weight (g)[b]	Daily 8-MOP intake (mg/kg b.w./day)
1	8-MOP 100 ppm+NNK	20	26.54±6.14	21.39±3.16
2	8-MOP 10 ppm+NNK	20	26.86±5.77	2.45±0.31
3	8-MOP 1 ppm+NNK	20	26.24±5.43	0.24±0.02
4	NNK alone	20	27.33±5.97	0
5	8-MOP 100 ppm+saline	20	28.22±2.53	23.95±2.70

[a] Number of mice examined.
[b] Mean±SD.

Table 2
Data for incidences and multiplicities of NNK-induced lung proliferative lesions in A/J mice treated with 8-MOP

Group	Treatment	No.[a]	Hyperplasia		Adenoma		Hyperplasia + adenoma	
			Incidence (%)[b]	Tumors/ mouse[c]	Incidence (%)	Tumors/ mouse	Incidence (%)	Tumors/ mouse
1	8-MOP 100 ppm + NNK	20	5/20 (25.0)[d]	0.25 ± 0.44[e]	10/20 (50.0)[f]	0.60 ± 0.68 [g]	13/20 (65.0)[d]	0.85 ± 0.75[e]
2	8-MOP 10 ppm + NNK	20	16/20 (80.0)	1.50 ± 1.00	14/20 (70.0)	1.35 ± 1.39	17/20 (85.0)	2.85 ± 1.73
3	8-MOP 1 ppm + NNK	20	15/20 (75.0)	1.55 ± 1.43	17/20 (85.0)	2.15 ± 1.53	19/20 (95.0)	3.70 ± 2.54
4	NNK alone	20	19/20 (95.0)	1.85 ± 1.18	15/20 (75.0)	1.85 ± 1.57	20/20 (100)	3.70 ± 2.23
5	8-MOP 100 ppm + saline	20	2/20 (10.0)	0.10 ± 0.31	1/20 (5.0)	0.05 ± 0.22	3/20 (15.0)	0.15 ± 0.37

[a] Number of mice examined.
[b] Number of mice observed each lesion (%).
[c] Mean ± SD.
[d] Significantly different from Group 4 by Fisher's exact probability test ($P < 0.01$).
[e] Significantly different from Group 4 by Student's-t test ($P < 0.0001$).
[f] Significantly different from Group 3 by Fisher's exact probability test ($P < 0.05$).
[g] Significantly different from Group 4 by Student's-t test ($P < 0.001$).

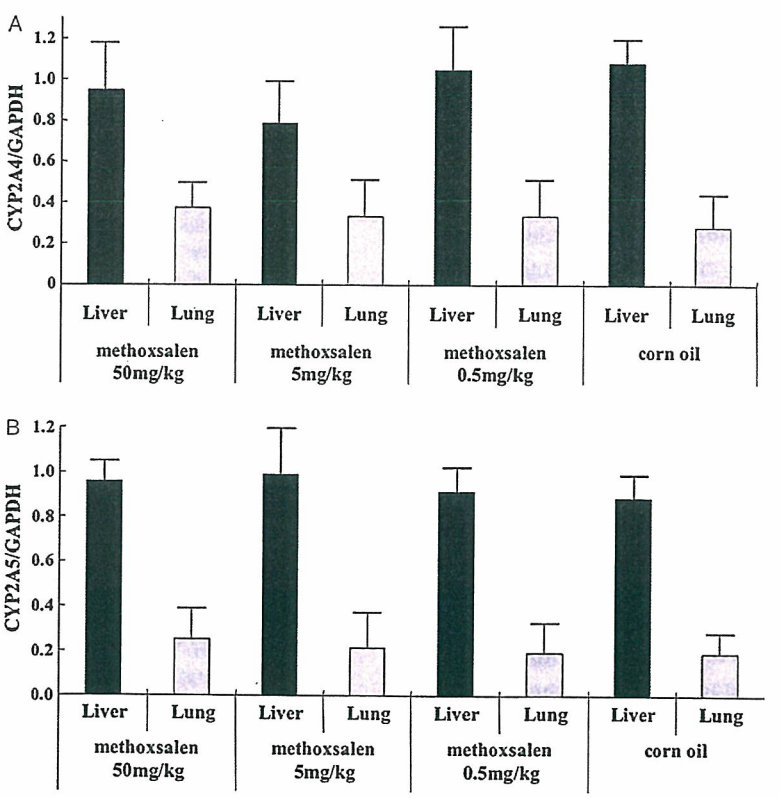

Fig. 2. Quantitative real-time RT-PCR analyses of mouse CYP2A4 and CYP2A5 mRNA expression in the livers and lungs. Data are mean ± SD values, normalized with respect to GAPDH.

tumors were 7.2–11.9 tumors/mouse [20–24]. In our previous study [19], multiplicity of NNK-induced lung adenomas and hyperplasia+adenomas were 5.97 and 8.16/mouse, respectively. In another unpublished study in our laboratory, the values were 13.4 and 15.6 tumors/mouse. However, in the present study, the corresponding figures were 1.85 and 3.70/mouse. It is difficult to explain these differences, but the basal diet used might be an important factor. In our previous study, we used Oriental MF diet (Oriental Yeast Co., Ltd, Tokyo, Japan) which is cereal based closed formula diet as the basal diet, whereas in the present study, we used Labo MR diet, another cereal-based closed formula diet. Hecht has reported that lung tumor multiplicity in NNK-treated mice is greater when maintained on the AIN-76A than the NIH-07 diet [20], respectively semi-synthesized and cereal based open formula diets. The suggestion was made that a component of the NIH-07 diet may inhibit tumor initiation by NNK. This is also as possible influence with our basal diets.

One other possibility is variation in viral infection. It is well established that bacteria or viruses play important roles in carcinogenesis in several organs. For example, H. pylori is considered a gastric carcinogen [25], the human papilloma virus causes cancer of the uterine cervix [26], and hepatitis B and C viruses causes hepatocellular carcinoma development [27,28]. Similarly, lung carcinogenesis may also be influenced by infection with viruses [29,30]. Furthermore, administration of antibiotics has been found to inhibit progression of rat lung carcinogenesis by suppressing chronic inflammation [31]. In the present study, mice were maintained under specific pathogen free (SPF) conditions, but in our previous study the animal laboratories were conventional (non-SPF).

8-MOP is a proven mechanism based inhibitor of human CYP2A6 [16] and mouse CYP2A4 and CYP2A5 [17], reducing enzyme activity. In the present study, we could not obtain any evidence that 8-MOP inhibits mRNA expression of the two isoforms. In conclusion, the results of this study showed clear dose dependent inhibitory effects of 8-MOP on NNK-induction of lung tumorigenesis in female A/J mice fed diet containing 8-MOP, apparently due to inhibition of activity of CYP2A4 and CYP2A5, rather than their mRNA expression.

Acknowledgements

We thank Ms Kyoko Hosokawa for her technical assistance and Dr Malcolm A. Moore for help in the preparation and critical reading of the manuscript. This study was supported in part by Grants-in-Aid for Cancer Research from the Ministry of Health, Labour and Welfare and the Ministry of Education, Science, Sports and Culture of Japan, and a Grant-in-Aid (No. 99-2) from the Organization for Pharmaceutical Safety and Research (OPSR) of Japan. We also gratefully acknowledge a Grant-in-Aid from the Core Research for Evolutional Science and Technology, and an SRF Grant for Biomedical Research in Japan.

References

[1] M.L. Janssen-Heijnen, J.W. Coebergh, The changing epidemiology of lung cancer in Europe, Lung Cancer 41 (2003) 245–258.
[2] I. Yoshimi, A. Ohshima, W. Ajiki, H. Tsukuma, T. Sobue, A comparison of trends in the incidence rate of lung cancer by histological type in the Osaka Cancer Registry, Japan and in the Surveillance, Epidemiology and End Results Program, USA, Jpn. J. Clin. Oncol. 33 (2003) 98–104.
[3] W.D. Travis, L.B. Travis, S.S. Devesa, Lung cancer, Cancer 75 (1995) 191–202.
[4] S.D. Stellman, J.E. Muscat, S. Thompson, D. Hoffmann, E.L. Wynder, Risk of squamous cell carcinoma and adenocarcinoma of the lung in relation to lifetime filter cigarette smoking, Cancer 80 (1997) 382–388.
[5] E.L. Wynder, D. Hoffmann, Smoking and lung cancer: scientific challenges and opportunities, Cancer Res. 54 (1994) 5284–5295.
[6] S.A. Belinsky, T.R. Devereux, J.F. Foley, R.R. Maronpot, M.W. Anderson, Role of the alveolar type II cell in the development and progression of pulmonary tumors induced by 4-(methylnitrosamino)-1-(3-pyridyl)-1-butanone in the A/J mouse, Cancer Res. 52 (1992) 3164–3173.
[7] N. Ariyoshi, M. Miyamoto, Y. Umetsu, H. Kunitoh, H. Dosaka-Akita, Y. Sawamura, et al., Genetic polymorphism of CYP2A6 gene and tobacco-induced lung cancer risk in male smokers, Cancer Epidemiol. Biomarkers Prev. 11 (2002) 890–894.
[8] M. Fujieda, H. Yamazaki, T. Saito, K. Kiyotani, M.A. Gyamfi, M. Sakurai, et al., Evaluation of CYP2A6 genetic polymorphisms as determinants of smoking behavior and tobacco-related lung cancer risk in male Japanese smokers, Carcinogenesis 2004.
[9] H. Kushida, K. Fujita, A. Suzuki, M. Yamada, T. Endo, T. Nohmi, T. Kamataki, Metabolic activation of *N*-alkylnitrosamines in genetically engineered Salmonella typhimurium expressing CYP2E1 or CYP2A6 together with human NADPH-cytochrome P450 reductase, Carcinogenesis 21 (2000) 1227–1232.

[10] H. Takeuchi, K. Saoo, M. Yokohira, M. Ikeda, H. Maeta, M. Miyazaki, et al., Pretreatment with 8-methoxypsoralen, a potent human CYP2A6 inhibitor, strongly inhibits lung tumorigenesis induced by 4-(methylnitrosamino)-1-(3-pyridyl)-1-butanone in female A/J mice, Cancer Res. 63 (2003) 7581–7583.

[11] R. Lindberg, B. Burkhart, T. Ichikawa, M. Negishi, The structure and characterization of type I P-450(15) alpha gene as major steroid 15 alpha-hydroxylase and its comparison with type II P-450(15) alpha gene, J. Biol. Chem. 264 (1989) 6465–6471.

[12] P. Honkakoski, J. Maenpaa, J. Leikola, M. Pasanen, R. Juvonen, M.A. Lang, et al., Cytochrome P4502A-mediated coumarin 7-hydroxylation and testosterone hydroxylation in mouse and rat lung, Pharmacol. Toxicol. 72 (1993) 107–112.

[13] P. Honkakoski, M. Negishi, The structure, function, and regulation of cytochrome P450 2A enzymes, Drug Metab. Rev. 29 (1997) 977–996.

[14] N.D. Felicia, G.K. Rekha, S.E. Murphy, Characterization of cytochrome P450 2A4 and 2A5-catalyzed 4-(methylnitrosamino)-1-(3-pyridyl)-1-butanone (NNK) metabolism, Arch. Biochem. Biophys. 384 (2000) 418–424.

[15] L.A. Peterson, S.S. Hecht, O6-methylguanine is a critical determinant of 4-(methylnitrosamino)-1-(3-pyridyl)-1-butanone tumorigenesis in A/J mouse lung, Cancer Res. 51 (1991) 5557–5564.

[16] E.D. Kharasch, D.C. Hankins, J.K. Taraday, Single-dose methoxsalen effects on human cytochrome P-450 2A6 activity, Drug Metab. Dispos. 28 (2000) 28–33.

[17] A.J. Draper, A. Madan, A. Parkinson, Inhibition of coumarin 7-hydroxylase activity in human liver microsomes, Arch. Biochem. Biophys. 341 (1997) 47–61.

[18] J. Maenpaa, H. Sigusch, H. Raunio, T. Syngelma, P. Vuorela, H. Vuorela, O. Pelkonen, Differential inhibition of coumarin 7-hydroxylase activity in mouse and human liver microsomes, Biochem. Pharmacol. 45 (1993) 1035–1042.

[19] D.L. Dungworth, S. Rittinghausen, L. Schwartz, J.R. Harkema, Y. Hayashi, B. Kittel, et al., Respiratory system and methothelium: lung in: U. Mohr et al. (Ed.), International Classification of Rodent Tumors: The Mouse, WHO/IARC, Lyon, 2001, pp. 116–131.

[20] S.S. Hecht, M.A. Morse, S. Amin, G.D. Stoner, K.G. Jordan, C.I. Choi, F.L. Chung, Rapid single-dose model for lung tumor induction in A/J mice by 4-(methylnitrosamino)-1-(3-pyridyl)-1-butanone and the effect of diet, Carcinogenesis 10 (1989) 1901–1904.

[21] J.Y. Hong, Z.Y. Wang, T.J. Smith, S. Zhou, S. Shi, J. Pan, C.S. Yang, Inhibitory effects of diallyl sulfide on the metabolism and tumorigenicity of the tobacco-specific carcinogen 4-(methylnitrosamino)-1-(3-pyridyl)-1-butanone (NNK) in A/J mouse lung, Carcinogenesis 13 (1992) 901–904.

[22] M.A. Morse, S.D. LaGreca, S.G. Amin, F.L. Chung, Effects of indole-3-carbinol on lung tumorigenesis and DNA methylation induced by 4-(methylnitrosamino)-1-(3-pyridyl)-1-butanone (NNK) and on the metabolism and disposition of NNK in A/J mice, Cancer Res. 50 (1990) 2613–2617.

[23] C.C. Conaway, D. Jiao, G.J. Kelloff, V.E. Steele, A. Rivenson, F.L. Chung, Chemopreventive potential of fumaric acid, *N*-acetylcysteine, *N*-(4-hydroxyphenyl) retinamide and beta-carotene for tobacco-nitrosamine-induced lung tumors in A/J mice, Cancer Lett. 124 (1998) 85–93.

[24] G. Yang, Z.Y. Wang, S. Kim, J. Liao, D.N. Seril, X. Chen, et al., Characterization of early pulmonary hyperproliferation and tumor progression and their inhibition by black tea in a 4-(methylnitrosamino)-1-(3-pyridyl)-1-butanone-induced lung tumorigenesis model with A/J mice, Cancer Res. 57 (1997) 1889–1894.

[25] The EUROGAST Study Group, An international association between *Helicobacter pylori* infection and gastric cancer, Lancet 341 (1993) 1359–1362.

[26] H. zur Hausen, Human papillomaviruses in the pathogenesis of anogenital cancer, Virology 184 (1991) 9–13.

[27] Y. Kubo, K. Okuda, M. Hashimoto, Y. Nagasaki, H. Ebata, Antibody to hepatitis B core antigen in patients with hepatocellular carcinoma, Gastroenterology 72 (1977) 1217–1220.

[28] I. Saito, T. Miyamura, A. Ohbayashi, H. Harada, T. Katayama, S. Kikuchi, et al., Hepatitis C virus infection is associated with the development of hepatocellular carcinoma, Proc. Natl Acad. Sci. USA 87 (1990) 6547–6549.

[29] R.M. Peck, G.J. Eaton, E.B. Peck, S. Litwin, Influence of Sendai virus on carcinogenesis in strain A mice, Lab. Anim. Sci. 33 (1983) 154–156.

[30] J.C. Theiss, G.D. Stoner, A.J. Kniazeff, Effect of reovirus infection on pulmonary tumor response to urethan in strain A mice, J. Natl Cancer Inst. 61 (1978) 131–134.

[31] M. Tsutsumi, H. Kitada, K. Shiraiwa, M. Takahama, T. Tsujiuchi, H. Sakitani, et al., Inhibitory effects of combined administration of antibiotics and anti-inflammatory drugs on lung tumor development initiated by *N*-nitrosobis(2-hydroxypropyl)amine in rats, Carcinogenesis 21 (2000) 251–256.

BIOLOGY OF REPRODUCTION 75, 352–359 (2006)
Published online before print 26 April 2006.
DOI 10.1095/biolreprod.106.051136

PSPC1, NONO, and SFPQ Are Expressed in Mouse Sertoli Cells and May Function as Coregulators of Androgen Receptor-Mediated Transcription[1]

Sho Kuwahara,[3] Asako Ikei,[3] Yusuke Taguchi,[3] Yoshiaki Tabuchi,[4] Nariaki Fujimoto,[5] Masuo Obinata,[6] Seiichi Uesugi,[3] and Yasuyuki Kurihara[2,3]

Department of Environment and Natural Sciences,[3] Graduate School of Environment and Information Sciences, Yokohama National University, Yokohama 240-8501, Japan
Division of Molecular Genetics Research,[4] Life Science Research Center, University of Toyama, Toyama 930-0194, Japan
Department of Developmental Biology,[5] Research Institute for Radiation Biology and Medicine, Hiroshima University, Hiroshima 734-8553, Japan
Department of Cell Biology,[6] Institute of Development, Aging and Cancer, Tohoku University, Sendai, 980-8575, Japan

ABSTRACT

In Sertoli cells of testis, androgen receptor-regulated gene transcription plays an indispensable role in maintaining spermatogenesis. Androgen receptor activity is modulated by a number of coregulators which are associated with the androgen receptor. Non-POU-domain-containing, octamer binding protein (NONO), a member of the DBHS-containing proteins, complexes with androgen receptor and functions as a coactivator for the receptor. Paraspeckle protein 1 alpha isoform (PSPC1, previously known as PSP1) and Splicing factor, proline- and glutamine-rich (SFPQ, previously known as PSF), other members of the DBHS-containing proteins, are also found in androgen receptor complexes, suggesting that these DBHS-containing proteins may cooperatively regulate androgen receptor-mediated gene transcription. We demonstrated that PSPC1, NONO, and SFPQ are coexpressed in Sertoli cell line TTE3 and interact reciprocally. The effect of the DBHS-containing proteins on the transcriptional activity was assessed using the construct containing androgen-responsive elements followed by a luciferase gene. The results showed that all the DBHS-containing proteins activate androgen receptor-mediated transcription, and PSPC1 is the most effective coactivator among them. Furthermore, we confirmed the presence of PSPC1, NONO, and SFPQ proteins in Sertoli cells of adult mouse testis sections. These observations suggest that PSPC1, NONO, and SFPQ form complexes with each other in Sertoli cells and may regulate androgen receptor-mediated transcriptional activity.

androgen receptor, gene regulation, Sertoli cells, spermatogenesis, testis

INTRODUCTION

Spermatogenesis is a multistep process leading to the generation of highly specialized spermatozoa. The developmental process begins with spermatogonia that are committed to further differentiation by undergoing two meiotic divisions, resulting in haploid round spermatids. During spermiogenesis, haploid spermatids undergo drastic morphological changes, including formation of the acrosome and the sperm flagellum, decrease of the nuclear size due to the unique DNA packaging, and exclusion of most of the cytoplasm [1]. The complexity of the differentiation process requires a highly specialized program of gene expression of male germ cells [2, 3]. For example, cAMP responsive element modulator (CREM) has been shown to play an important role in germ cell-specific transcription by binding to CRE sequences [4, 5], and Poly (A) polymerase beta (PAPOLB) is known to adjust the timing of haploid-specific translation by controlling the cytoplasmic mRNA polyadenylation [6].

However, the endogenous gene expression program of male germ cells is not sufficient for spermatogenesis, and support from nearby Sertoli cells is indispensable. Throughout spermatogenesis, Sertoli cells interact directly with germ cells within the seminiferous tubules. Sertoli cells regulate highly organized and precisely synchronized germ cell development by nourishing germ cells via their secretion products [7–9]. These controls by Sertoli cells are also regulated by external stimuli. Androgen and androgen receptor (AR)-mediated gene transcription are important for the Sertoli cell functions [2, 10]. Mice lacking AR in Sertoli cells show spermatogenic arrest, which results in azoospermia and infertility [11, 12]. Thus, AR-mediated transcription in Sertoli cells plays an indispensable role in spermatogenesis.

AR belongs to the nuclear receptor superfamily that includes receptors for thyroid hormone, retinoic acid, estrogen, progesterone, glucocorticoid, and other hormones [13]. AR forms a homodimer and binds to androgen-responsive elements in promoters/enhancers of AR-driven genes. AR is composed of N-terminal transactivation domain (NTD), DNA-binding domain (DBD), and ligand-binding domain (LBD) at the C-terminus. NTD possesses an activation function domain 1 (AF-1) and is involved in making contact with the general transcriptional machinery [14–16]. The transcriptional activity of AR is modulated by coregulators, which include coactivators that enhance AR transactivation and corepressors that suppress AR transactivation [17–19].

Non-POU-domain-containing, octamer binding protein (NONO) is known as one of the coregulators of AR. NONO interacts directly with the AR AF-1 domain and acts as a coactivator [20, 21]. NONO contains a DBHS (Drosophila behavior, human splicing) domain characterized by two tandem RNA recognition motifs (RRMs) and a helix-turn-helix (HTH) DNA binding domain. In mammals, two other DBHS-

[1]Supported by grants from the Ministry of Education, Sports, Culture, Science and Technology of Japan (MEXT) to Y.K.
[2]Correspondence: Yasuyuki Kurihara, Department of Environment and Natural Sciences, Graduate School of Environment and Information Sciences, Yokohama National University, Tokiwa-dai, Hodogaya, Yokohama 240-8501, Japan. FAX: 81 45 339 4263;
e-mail: kurihara@ynu.ac.jp

Received: 23 January 2006.
First decision: 1 March 2006.
Accepted: 20 April 2006.
© 2006 by the Society for the Study of Reproduction, Inc.
ISSN: 0006-3363. http://www.biolreprod.org

containing proteins, Paraspeckle protein 1 (PSPC1, previously known as PSP1) and Splicing factor, proline- and glutamine-rich (SFPQ, previously known as PSF), have been reported [22, 23]. PSPC1 has two isoforms, alpha (referred to as PSPC1 in this paper) and beta, produced by alternative splicing. It has been reported that DBHS-containing proteins regulate nuclear receptors, such as progesterone receptor [24] and thyroid hormone receptor [25], and also participate in mRNA regulation in the nucleus, including splicing [26, 27], 3′-end cleavage [27, 28], and nuclear retention of edited RNA [29]. Since DBHS-containing proteins are identified in RNA-transporting granules [30], it is likely that these proteins also participate in RNA metabolism in the cytoplasm. In addition, DBHS-containing proteins are reported to be involved in activation of DNA topoisomerase I [31] and DNA double-strand break rejoining [32]. Therefore, these proteins are regarded as multifunctional proteins involved in various aspects of gene expression. In many cases, NONO and SFPQ are copurified [20, 27–40], suggesting that these proteins may control gene expression as a complex. We have previously confirmed the direct interaction between PSPC1 and NONO, and SFPQ by coimmunoprecipitation experiments and yeast two-hybrid assays [41], indicating that the DBHS-containing proteins interact reciprocally.

We have sought to define expression and function of DBHS-containing proteins in testis, and to elucidate the biological significance of these proteins in spermatogenesis. In this paper, we have shown the expression of the DBHS-containing proteins and reciprocal complex formations in the Sertoli cell line TTE3. These proteins enhanced AR-mediated transactivation, and we confirmed the expression of the DBHS-containing proteins in the Sertoli cells of adult mouse testis. These observations suggest that the DBHS-containing proteins may be involved in spermatogenesis by regulating AR-mediated transcription in the Sertoli cells.

MATERIALS AND METHODS

Plasmids, Cells, and Mice

The expression plasmids for Myc-tagged DBHS-containing proteins (pMyc-CMV-2-Pspc1, pMyc-CMV-2-Nono, and pMyc-CMV-2-Sfpq) were prepared by subcloning mouse *Pspc1alpha*, mouse *Nono*, and mouse *Sfpq* cDNAs (GenBank accession numbers: NM_025682, NM_023144 and NM_023603) into the pMyc-CMV-2 vector (Clontech). A PSPC1 RRM mutant (F118A, F120A, K197A, F199A), which did not bind to RNA, was generated as described previously [42] and cloned into pMyc-CMV-2. By using the same method, the expression plasmids for a NONO RRM mutant (pMyc-CMV-2-Nono RRM mutant, F113A, F115A, K192A, I194A) and a SFPQ RRM mutant (pMyc-CMV-2-Sfpq RRM mutant, F326A, F328A, K405A, I407A) were also generated. The expression vector for androgen receptor pSG5-hAR and p(ARE)$_2$-luc plasmid containing two consensus androgen-responsive elements were described earlier [43].

COS-1 cells were cultured in Dulbecco modified Eagle medium (DMEM)(Sigma) supplemented with 10% Donor Calf Serum (DCS) (Thermotrace) and maintained at 37°C in an atmosphere of 5% CO_2. TTE3 cells were cultured in DMEM containing 10% DCS on collagen type I precoated dishes (Celltight C-1, Sumitomo Bakelite) at the permissive temperature of 33°C or nonpermissive temperature of 37°C in an atmosphere of 5% CO_2.

Nine-week-old male BALB/cAJcl mice were purchased from CLEA Japan. Animal experiments were conducted in accordance with the National Institutes of Health standards established in the Guidelines for the Care and Use of Experimental Animals.

Mouse Monoclonal Antibody Production

Synthetic peptides corresponding to amino acids 505–523 in mouse PSPC1 (CFGRGSQGGNFEGPNKRRRY), 453–464 in mouse NONO (CPPAFNRPAPGAE), and 681–699 in mouse SFPQ (CAGYGRGREEYEGPNKKPRF) were purchased from BIO SYNTHESIS. These peptides, conjugated with KLH (Pierce), were injected twice at a 1-wk interval into BALB/cAJcl mice. Three days after the second boost, the lymph node cells were fused with the myeloma line P3U1. The culture media were screened by ELISA and following immunoblotting. The cells from the positive wells were cloned by the standard limiting dilution technique. Anti-PSPC1 (clone 1L4), anti-NONO (clone NC5), and anti-SFPQ (clone FC23) mouse monoclonal antibodies were used in this study.

Immunoblotting

Fifteen μg of TTE3 cell lysates prepared as described previously [41] were analyzed on 8% SDS-polyacrylamide gels and blotted onto Immobilon-P membrane (Millipore). After saturation with 5% skim milk (Difco) in Tris-buffered saline (20 mM Tris-HCl pH 7.6, 137 mM NaCl) containing 0.1% Tween-20 for 1 h at room temperature, membranes were incubated with a 1:40 dilution of antibodies to either PSPC1, NONO, or SFPQ followed by an incubation with a 1:10000 dilution of HRP-conjugated goat anti-mouse IgG (ZYMED). Enzymatic activities were detected by ECL substrate (Amersham Biosciences).

Immunocytochemistry

TTE3 cells were fixed in 4% paraformaldehyde in PBS for 20 min and for an additional 30 min in methanol. After washing with PBS, coverslips were blocked with 10% goat serum. Cells were incubated with a 1:10 dilution of anti-PSPC1, anti-NONO, or anti-SFPQ antibody respectively for 1.5 h at room temperature. After washing three times with PBS, the cells were incubated with a 1:100 dilution of Alexa Fluor 546 goat anti-mouse IgG (Invitrogen), for 30 min. The expression of proteins was visualized by fluorescence microscopy (Olympus).

Immunoprecipitation

For immunoprecipitation analysis, TTE3 cells (1.8×10^7 cells) were harvested and lysed in 4.8 ml of lysis buffer (50 mM Tris-HCl pH 7.4, 150 mM NaCl, 5 mM EDTA, 50 mM NaF, 0.5% NP-40, 1 mM Na_3VO4, 1 mM PMSF, 1 μg/ml aprotinin, 1 μg/ml pepstatin, 1 μg/ml leupeptin, 1 mM DTT) with or without 10 μg/ml RNase A and incubated at 4°C for 30 min followed by centrifugation at 15,000 rpm for 15 min. The resulting supernatants were decanted into fresh tubes and preabsorbed with Protein-A agarose beads (SIGMA) for 30 min followed by incubation with anti-PSPC1, anti-NONO, anti-SFPQ, or anti-Myc (9E10) antibody coupled to Protein A-agarose beads for 2 h. The immunoprecipitates were washed three times with lysis buffer. Immunoprecipitates were immunoblotted with each antibody.

Luciferase Assay

COS-1 cells were transiently transfected by the calcium phosphate precipitate method with 0.2 μg of p(ARE)$_2$-luc plasmid, 0.1 μg of pSG5-hAR, 0.3 μg of PSPC1, NONO, or SFPQ expression vector. The total amount of vector added to each well was adjusted by adding an empty vector pMyc-CMV-2. Six hours after transfection, the media were replaced with fresh media containing 0.2% DCS. Dihydrotestosterone (DHT, 10^{-9} M) ligand was added and cells were incubated for an additional 12 h. Luciferase activities were determined as described previously [44] using a TD-20/20 luminometer (Turner Designs). Each plasmid was assayed in triplicate at least three different times. pRL-tk (Promega) was cotransfected to normalize transfection efficiencies. All the data were analyzed by Student *t*-test using Microsoft Excel. A P value of less than 0.05 was considered to be statistically significant.

RT-PCR Analysis

COS-1 cells were transfected and treated with DHT as done in the luciferase assay with the exception that cells were cultured in 90 mm dishes. Cells were harvested, lysed in IP buffer (50 mM Tris-HCl pH 7.5, 200 mM NaCl, 5 mM EDTA, 1% Triton-X100, 0.5% NP-40, 250 mM sucrose, 1 mM PMSF, 1 μg/ml aprotinin, 1 μg/ml pepstatin, 1 μg/ml leupeptin, 50 mM NaF, 1 mM Na_3VO4, 1 mM DTT, 10 U/ml RNase inhibitor (TOYOBO), and incubated at 4°C for 20 min followed by centrifugation at 15,000 rpm for 15 min. The supernatants were decanted into fresh tubes and preabsorbed with Protein G-Sepharose 4 Fast Flow (Amersham Biosciences) for 30 min followed by incubation with anti-Myc monoclonal antibody (9E10) or anti-HA monoclonal antibody (12CA5) coupled to Protein G-Sepharose 4 Fast Flow for 1 h. After washing the immunoprecipitates five times with IP buffer, RNA was purified with an RNeasy Mini Kit (QIAGEN). Eluted RNA was reverse-transcribed using a Sensiscript RT Kit (QIAGEN) with the luciferase rv primer, (5′-CGAGTGTAGTAAACATTCCAAAACCGTGATGG-3′), and amplified

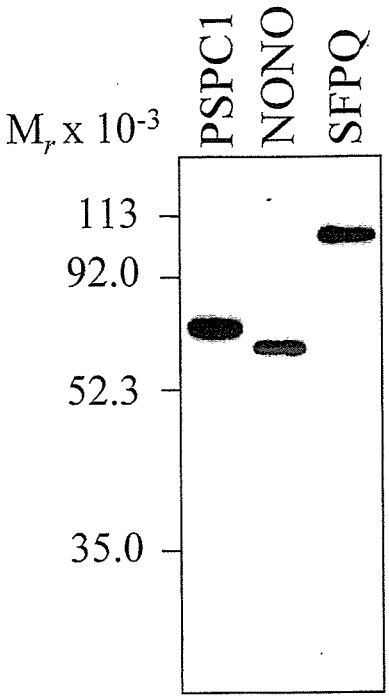

FIG. 1. PSPC1, NONO, and SFPQ expressed in Sertoli cell line TTE3. TTE3 cell extracts were electrophoresed on SDS-PAGE gels, transferred onto polyvinylidene fluoride membranes, and incubated with anti-PSPC1, anti-NONO, or anti-SFPQ antibodies.

using SP-Taq DNA polymerase (Hokkaido System Science) with the luciferase fw primer, (5′-CTAAAACGGATTACCAGGGATTTCAGTCGATG-3′), and the luciferase rv primer.

Immunohistochemistry

Testes were removed from BALB/cAJcl mice deeply anesthetized with Ketalar 50 (Sankyo) and fixed overnight in Bouin fixative. The testes were embedded in paraffin and cut into 8-μm sections. After deparaffinization and rehydration by xylene and serial dilutions of aqueous ethanol, the slides were immersed in sodium citrate buffer pH 6.0 and heated for 10 min at 121°C for antigen retrieval. The slides were washed in PBS and permeabilized with 0.2% Triton X-100 in PBS for 30 min at room temperature. After blocking with 10% goat serum and 1% BSA, cells were incubated with a 1:10 dilution of anti-PSPC1, anti-NONO, or anti-SFPQ antibody or a 1:300 dilution of anti-WT1 rabbit polyclonal antibody (Santa Cruz Biotechnology), in 2% goat serum and 1% BSA in PBS overnight at 4°C. Subsequently, slides were washed, incubated with a 1:100 dilution of Alexa Fluor 488 F(ab′)$_2$ fragment of goat anti-mouse IgG (H+L) (Invitrogen) and goat anti-rabbit IgG (H+L)-TRITC (Zymed) in 10% goat serum and 1% BSA in PBS for 2 h at room temperature, and counterstained with DAPI (4′,6-diamidino-2-phenylindole, dihydrochloride).

RESULTS

Monoclonal Antibody Production

Previously we reported that rabbit polyclonal antibody raised against bacterially expressed recombinant PSPC1 recognizes both of PSPC1alpha and its splicing variant PSPC1beta, and kidney expresses PSPC1beta exclusively [41]. However, mass spectrometric analysis showed that the immunoprecipitates from kidney actually contained one isoform of SEPT4 (previously known as M-Septin) [45], but not PSPC1beta (data not shown). These two proteins have a similar molecular mass (PSPC1beta; 45 kDa, SEPT4; 44 kDa) and share antigenic determinant EELRRXQE in PSPC1 (369–376) and SEPT4 (359–366). To avoid cross-reaction, we designed a new synthetic peptide specific to PSPC1, immunized BALB/cAJcl with the peptide, and developed a mouse anti-PSPC1 monoclonal antibody. On Western blotting, this antibody recognized a single band of 59-kDa protein in testis and kidney (see Supplemental Figure 1, available online at www.biolreprod.org). Similarly, we developed anti-NONO and anti-SFPQ mouse monoclonal antibodies. We performed a peptide competition study to verify the specificities, and the results indicated that these antibodies specifically recognized PSPC1, NONO, or SFPQ and had no cross-reactivity with other DBHS-containing proteins (see Supplemental Figure 2, available online at www.biolreprod.org). Moreover we carried out mass spectrometric analysis of the peptides immunoprecipitated from mouse testis extracts by the antibodies. MALDI profiles revealed that anti-PSPC1 antibody immunoprecipitated PSPC1 protein, anti-NONO antibody immunoprecipitated NONO protein, and anti-SFPQ antibody immunoprecipitated SFPQ protein (see Supplemental Table 1, available online at www.biolreprod.org). These data confirmed the antigenic specificities of monoclonal antibodies, and these antibodies were used for the following analysis.

DBHS-Containing Proteins Are Expressed in Sertoli Cell Line TTE3

NONO interacts with AR and enhances transcriptional activity, and PSPC1 and SFPQ, other members of the DBHS-containing proteins, coprecipitate with AR [20]. These data suggest that PSPC1 and SFPQ may also modulate AR activity. Androgen and AR-dependent gene transcription in Sertoli cells are essential for maintaining normal spermatogenesis. We investigated whether DBHS-containing proteins are expressed in Sertoli cell line TTE3, which is a conditionally immortalized testicular Sertoli cell line from transgenic mice bearing the temperature-sensitive simian virus 40 large T antigen gene [46]. Whole-cell extracts from TTE3 cells were separated by SDS-PAGE, transferred to polyvinylidene fluoride membrane, and probed with anti-PSPC1, anti-NONO, or anti-SFPQ antibody. PSPC1, NONO and SFPQ were expressed abundantly in TTE3 cells (Fig. 1). Next, we examined the intracellular distributions of DBHS-containing proteins in TTE3 cells. TTE3 cells were cultured on coverslips, fixed, and immunostained with each antibody. Strong expressions of PSPC1, NONO, and SFPQ were detected in the nucleus while faint signals for PSPC1 and NONO and an intensive signal for SFPQ were also observed in the cytoplasm (Fig. 2).

Endogenous DBHS-Containing Proteins in TTE3 Cells Form Complexes with Each Other

Complex formation among DBHS-containing proteins is a controversial issue. Fox et al. reported that PSPC1-NONO and NONO-SFPQ complexes were observed in HeLa cells, but PSPC1-SFPQ complex was not [42]. In our previous paper, all reciprocal interactions were shown by coimmunoprecipitation assays of overexpressed DBHS-containing proteins, and yeast two-hybrid assays [41]. Therefore, we investigated complex formation among endogenous DBHS-containing proteins in TTE3 cells. DBHS-containing proteins were immunoprecipitated with anti-PSPC1, anti-NONO, or anti-SFPQ antibody from TTE3 cells, and the immunoprecipitants were subjected to Western blotting with appropriate antibodies. PSPC1 coimmunoprecipitated with NONO and SFPQ, and NONO and SFPQ behaved similarly (Fig. 3). Addition of RNase to the cell extracts did not alter the immunoprecipitation, indicating that the interaction between DBHS-containing proteins is a direct protein-protein interaction. DAZAP1, which is abundantly expressed in testis, did not coimmunoprecipitate with DBHS-

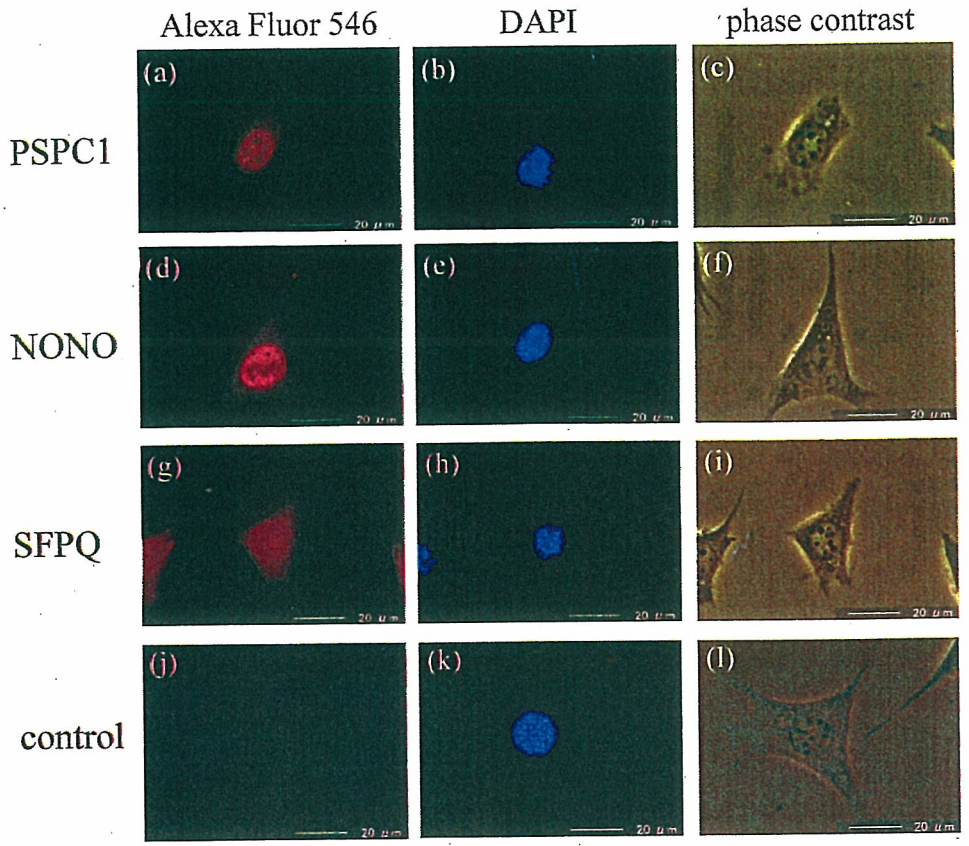

FIG. 2. Localization of the DBHS-containing proteins in TTE3 cells. TTE3 cells were grown on coverslips and labeled for immunofluorescence with antibody to PSPC1 (**a**), NONO (**d**), or SFPQ (**g**). The cells treated only with the secondary antibody were used as negative controls (**j**). **b**, **e**, **h**, and **k**) Nuclear staining by DAPI for the same samples in **a**, **d**, **g**, and **j**, respectively. **c**, **f**, **i**, and **l**) Phase contrast microscopy for the same samples in **a**, **d**, **g**, and **j**, respectively.

containing proteins [47, 48], showing that the interactions are significant. Interestingly, the amount of PSPC1 precipitated with anti-PSPC1 antibody was about the same as the amounts of NONO and SFPQ coimmunoprecipitated with PSPC1. Immunoprecipitations by anti-NONO antibody and anti-SFPQ antibody showed similar tendencies.

DBHS-Containing Proteins Regulate AR-Mediated Transcription

To investigate whether DBHS-containing proteins affect AR-mediated transcription, we planned to perform a luciferase assay with TTE3 cells. Although we tried various transfection reagents and transfection protocols repeatedly, transfection efficiency was extremely low. Therefore the luciferase assay with COS-1 cells using a reporter plasmid containing androgen-responsive elements was performed. COS-1 cells were transfected with expression plasmids for AR and DBHS-containing proteins and reporter plasmids, and treated with DHT. NONO enhanced the transactivation function of AR as previously reported [20, 21], and PSPC1 and SFPQ also enhanced the AR function. PSPC1 showed the highest transactivation of the reporter gene while NONO and SFPQ showed equally lower transactivation (Fig. 4a). DBHS-containing proteins are RNA binding proteins that share RNA recognition motifs (RRMs). We tested whether DBHS-containing proteins bind to luciferase mRNA. COS-1 cells were transfected, treated with DHT as done in the luciferase assay, and harvested. Myc-PSPC1, Myc-NONO, or Myc-SFPQ was immunoprecipitated from cell lysates with anti-Myc antibody. RT-PCR was performed for the immunoprecipitant as template with luciferase-specific primers, and weak binding of DBHS-containing proteins to luciferase mRNA was observed (Fig. 4b, lane 4). Next, to address the question whether the enhancement of luciferase activity is influenced by post-transcriptional regulation, the RRM mutants, in which the RNA binding activity was abolished without disrupting the overall structure of the RRM domain, were constructed according to the procedure of Fox et al. [42], and luciferase assays were performed. These mutants did not show RNA binding activity (Fig. 4b, lane 2) but did show activated AR-mediated transcription as well as the wild type DBHS-containing proteins in the luciferase assay (Fig. 4a). These data demonstrate that the enhancement of luciferase activity is mediated by transcriptional regulation, not by post-transcriptional regulation.

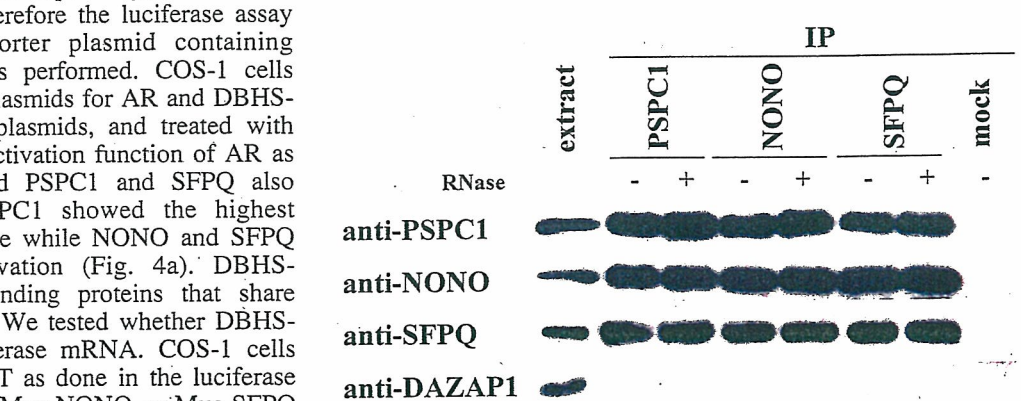

FIG. 3. DBHS-containing proteins interact reciprocally. TTE3 cell lysates treated with RNase or untreated lysates were subjected to immunoprecipitation with anti-PSPC1, anti-NONO, anti-SFPQ, or anti-Myc (9E10, for negative control) antibody. Western blotting was performed with whole extracts and immunocomplexes using an appropriate antibody.

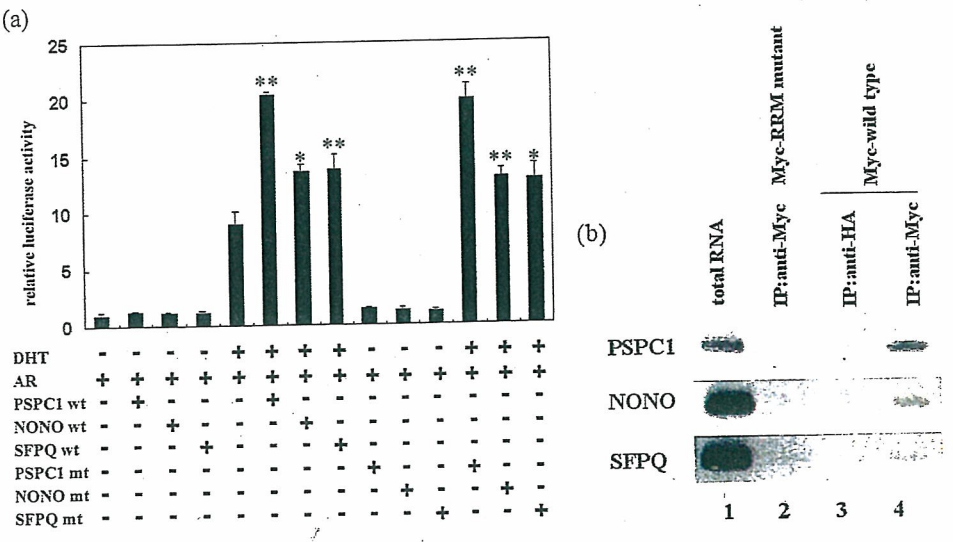

FIG. 4. DBHS-containing proteins regulate androgen receptor-mediated transcription. a) COS-1 cells were cotransfected with $p(ARE)_2$-luc (a luciferase reporter plasmid containing androgen-responsive elements), expression vector containing AR, and wild type (wt) or RRM mutant (mt) DBHS-containing protein expression vector in the absence (−) or presence (+) of dihydrotestosterone (DHT). The bars represent the mean ± SD. * $P < 0.05$ vs. control experiments without DBHS-containing protein expression vector; ** $P < 0.01$ vs. control experiments without DBHS-containing protein expression vector. b) DBHS-containing protein RRM mutants do not bind to luciferase mRNA. COS-1 cells were transfected with Myc-tagged DBHS-containing protein RRM mutant or Myc-tagged DBHS-containing protein wild type expression vectors as luciferase assay. Cell lysates were subjected to immunoprecipitation with anti-Myc or anti-HA antibody. RT-PCR was performed with immunoprecipitants as templates and luciferase-specific primers. Total cell RNA was assayed as a positive control.

DBHS-Containing Proteins Are Expressed in Sertoli Cells of Testis

DBHS-containing proteins were expressed in Sertoli cell line TTE3, along with activated androgen receptor-mediated transcription. We next examined the expression of DBHS-containing proteins in Sertoli cells of testis. Adult mouse testis sections were immunostained with anti-PSPC1, anti-NONO, or anti-SFPQ antibody. Anti-WT1 antibody was used as a marker to identify the Sertoli cells [49]. The expression of each DBHS-containing protein in seminiferous tubules displayed a distinct profile. The germ cells expressed PSPC1 and SFPQ, but not NONO (Fig. 5b, 5l and 5g, respectively). The signals of all DBHS-containing proteins were detected in the cells adjacent to the basal membrane of the seminiferous tubule. These cells also expressed WT1 (Fig. 5a, 5f and 5k), demonstrating that all the DBHS-containing proteins are expressed in the Sertoli cells.

DISCUSSION

In this study, we showed that all of the three DBHS-containing proteins are expressed in mouse Sertoli cell line TTE3, and interact reciprocally. These proteins enhanced AR-mediated transactivation. Expression of the DBHS-containing proteins in Sertoli cells of adult mouse testis suggests that the DBHS-containing proteins may play roles in spermatogenesis by regulating AR-mediated transcription in Sertoli cells.

First, we showed the abundant and equivalent expressions of all the DBHS-containing proteins in Sertoli cell line TTE3. However, in germ cells, PSPC1 and SFPQ were expressed abundantly, but NONO was not detected. In HeLa cells, Fox et al. reported that NONO is expressed at higher levels than that for PSPC1 [42]. Although expression of SFPQ is confirmed in various tissues and cell lines [50, 51], expression levels of NONO are different among tissues and cell lines [52]. PSPC1 is expressed abundantly in mouse testis [41]. These data indicate that at least expression levels of PSPC1 and NONO are different depending on tissues and cell types.

The transcriptional activity of AR is modulated by various coregulators, which include coactivators and corepressors. Luciferase assay using a reporter plasmid containing androgen-responsive elements indicated that all the DBHS-containing proteins enhance the transcription mediated by AR. PSPC1 showed the highest transactivation of the reporter gene, and NONO and SFPQ showed equal transactivation. These data suggest that DBHS-containing proteins are coactivators of AR. The coregulators can be divided into two major types. Type I coregulators, such as HMGB1 and HMGB2 [53] and CMTM2A [54], function primarily with the nuclear receptor at the target gene promoter to facilitate DNA occupancy, chromatin remodeling, or the recruitment of general transcription factors associated with the RNA polymerase II holocomplex. Type II coregulators, such as FLNC [55] and PAK6 [56], contribute to AR protein stability in the presence of ligands or influence the subcellular distribution of AR [17–19]. Although the molecular mechanism of AR transactivation by the DBHS-containing proteins remains elusive, the DBHS-containing proteins are known to have a DNA binding domain [23, 41], and we confirmed the expression of these proteins in the nucleus of the TTE3 cell line. It was previously reported that NONO enhances the association of transcription factors to their target DNA [57], suggesting that the DBHS-containing proteins enhance the association of AR to their targets, like HMGB1 and HMGB2 enhance the binding of AR, progesterone receptor, and glucocorticoid receptors to their target DNA and enhance the transactivation [53]. Alternatively, DBHS-containing proteins might activate transactivation of AR by stimulating DNA topoisomerase I to relieve torsional strain, and this is supported by the observation that NONO and SFPQ interact with DNA topoisomerase I and activate its enzymatic activity [31]. Thus we speculate that DBHS-containing proteins belong to the Type I coregulators that functions primarily at the target gene promoter site.

DBHS-containing proteins are known not only to regulate transcription but also to bind directly to RNA for post-transcriptional regulation. DBHS-containing proteins are also known to be involved in splicing, polyadenylation, nuclear retention of edited RNA, and transport of mRNA [23, 26–30]. In TTE3 cells, SFPQ was expressed not only in the nucleus but also in the cytoplasm, and weak expression of PSPC1 and NONO was observed in the cytoplasm. We also found weak but significant expression of PSPC1 in the cytoplasm of germ

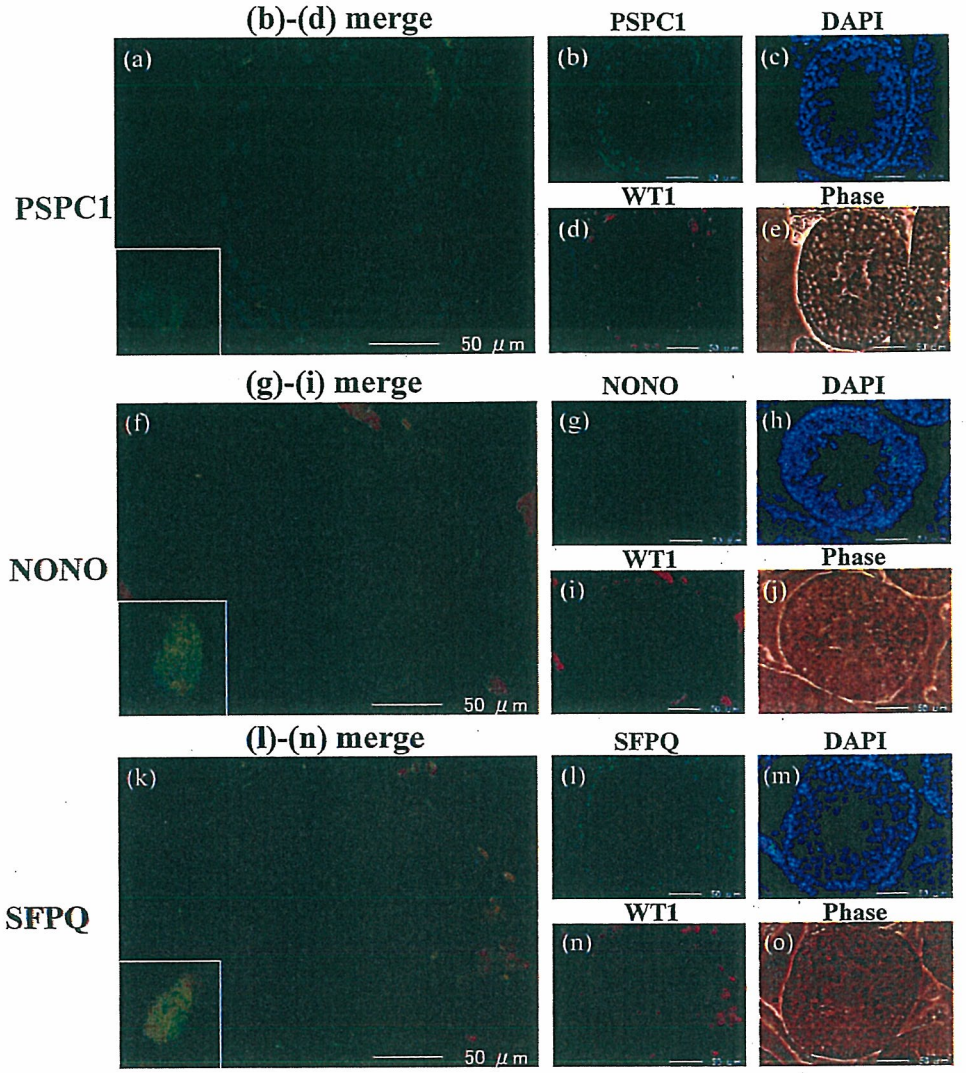

FIG. 5. Expression of DBHS-containing proteins in mouse adult testis. Sections of adult mouse testis were immunostained with anti-PSPC1 (**b**), anti-NONO (**g**), or anti-SFPQ (**l**) antibody. **d**, **i**, and **n**) Immunostaining with anti-WT1 rabbit polyclonal antibody for the same samples in **b**, **g**, and **l**, respectively. **c**, **h**, and **m**) Nuclear staining by DAPI for the same samples in **b**, **g**, and **l**, respectively. **e**, **j**, and **o**) Phase contrast microscopy for the same samples in **b**, **g**, and **l**, respectively. **a**) Merged image of **b-d**. **f**) Merged image of **g-i**. **k**) Merged image of **i-n**. The insets in **a**, **f**, and **k** show high magnifications of Sertoli cells.

cells (data not shown), suggesting that DBHS-containing proteins function also in the cytoplasm. From these findings, we speculate that DBHS-containing proteins may regulate not only transcription but also RNA metabolism such as splicing, mRNA export, and RNA nuclear retention. The DBHS-containing proteins may maintain spermatogenesis by activating AR-mediated transcription and regulating the transcribed mRNA both in the nucleus and cytoplasm of Sertoli cells.

Fox et al. reported that PSPC1 interacts with NONO, and not with SFPQ in HeLa cells [42]. However, we previously showed the interaction between overexpressed PSPC1 and NONO, and also between PSPC1 and SFPQ [41]. In this study, we investigated the complex formation among the endogenous DBHS-containing proteins in TTE3 cells, and observed all combinations of the interactions among PSPC1, NONO, and SFPQ. It has been reported that all the DBHS-containing proteins are found in the protein complex with the AR AF-1 domain [20]. Moreover, our preliminary proteomic analysis demonstrated that anti-PSPC1 antibody immunoprecipitates NONO and SFPQ together with PSPC1 in testis extract, and yeast two-hybrid assays using PSPC1 as a bait protein showed the interaction of PSPC1 with NONO and SFPQ (data not shown). Therefore PSPC1 actually interacts with both NONO and SFPQ. We assume that the inconsistency between the data by Fox et al. and by us may come from the difference in the interacting partner in the cell line used, not only from the difference in expression levels of the DBHS-containing proteins. If we assume that PSPC1 forms only heterodimers with NONO or SFPQ, PSPC1 should immunoprecipitate most abundantly among these proteins. However, the amount of PSPC1 precipitated with anti-PSPC1 antibody was almost the same as those of NONO and SFPQ coimmunoprecipitated with PSPC1. Immunoprecipitations by anti-NONO antibody and anti-SFPQ antibody also showed similar tendencies. These results raise the possibility that the DBHS-containing proteins may form multimers. It was previously reported that Hrp65 protein, *Chironomus tentans* homolog of the PSPC1/NONO/SFPQ family, can self-associate, and most of the Hrp65 protein are in complexes that consist of three to six Hrp65 protein molecules [58], suggesting that PSPC1, NONO, and SFPQ also form large complexes by interacting reciprocally. DBHS-containing proteins are known not only to regulate transcription but also to be involved in multiple regulations including RNA metabolism [23, 26–30] and DNA metabolism [31, 32]. It is likely that the differences in the composition of the DBHS-containing protein complex bring about functional diversity of DBHS-containing proteins.

We confirmed the expressions of all the DBHS-containing proteins in Sertoli cells of adult mouse testis, and these proteins exhibited enhancement of transactivation of AR. PSPC1 and SFPQ were expressed also in germ cells. Because germ cells do not express AR, PSPC1 and SFPQ expressed in germ cells may

function in an androgen-independent mechanism. It is known that a number of coactivators function as general coactivators for transcription mediated by nuclear receptors. For example RBM14 is known to activate glucocorticoid receptor-, estrogen receptor-, and thyroid hormone receptor-mediated transcription [59]. It has been reported that SFPQ regulates progesterone receptor, thyroid hormone receptor and retinoic acid receptor, suggesting that SFPQ is a general coregulator of nuclear receptors [24, 25]. In germ cells, several specific nuclear receptors are expressed [60, 61]. PSPC1 and SFPQ may regulate transcription mediated by another nuclear receptor in germ cells. Sertoli cells regulate highly organized and precisely synchronized germ cell development by nourishing the germ cells via their secretion products. Activity of AR-mediated transcription in Sertoli cells is regulated by multiple coregulators. Our present study suggests that the DBHS-containing proteins are coactivators of AR transactivation in Sertoli cells and may be determinants of androgen activity during spermatogenesis. In conclusion, PSPC1, NONO, and SFPQ may support spermatogenesis by regulating androgen receptor-mediated transcription in Sertoli cells.

ACKNOWLEDGMENTS

We thank Dr. Naohito Nozaki for antibody production, and M.S. Atsushi Kawaguchi for his helpful discussion.

REFERENCES

1. Russell LD, Ettlin RA, Sinha Hikim AP, Clegg ED. Histological and Histopathological Evaluation of the Testis. Clearwater, FL: Cache River Press; 1990:1–40.
2. Maclean JA 2nd, Wilkinson MF. Gene regulation in spermatogenesis. Curr Top Dev Biol 2005; 71:131–197.
3. Tanaka H, Baba T. Gene expression in spermiogenesis. Cell Mol Life Sci 2005; 62:344–354.
4. Monaco L, Kotaja N, Fienga G, Hogeveen K, Kolthur US, Kimmins S, Brancorsini S, Macho B, Sassone-Corsi P. Specialized rules of gene transcription in male germ cells: the CREM paradigm. Int J Androl 2004; 27:322–327.
5. Kimmins S, Kotaja N, Davidson I, Sassone-Corsi P. Testis-specific transcription mechanisms promoting male germ-cell differentiation. Reproduction 2004; 128:5–12.
6. Kashiwabara S, Noguchi J, Zhuang T, Ohmura K, Honda A, Sugiura S, Miyamoto K, Takahashi S, Inoue K, Ogura A, Baba T. Regulation of spermatogenesis by testis-specific, cytoplasmic poly(A) polymerase TPAP. Science 2002; 298:1999–2002.
7. Mruk DD, Cheng CY. Sertoli-Sertoli and Sertoli-germ cell interactions and their significance in germ cell movement in the seminiferous epithelium during spermatogenesis. Endocr Rev 2004; 25:747–806.
8. Griswold MD. The central role of Sertoli cells in spermatogenesis. Semin Cell Dev Biol 1998; 9:411–416.
9. Syed V, Hecht NB. Disruption of germ cell-Sertoli cell interactions leads to spermatogenic defects. Mol Cell Endocrinol 2002; 186:155–157.
10. Dohle GR, Smit M, Weber RF. Androgens and male fertility. World J Urol 2003; 21:341–345.
11. Chang C, Chen YT, Yeh SD, Xu Q, Wang RS, Guillou F, Lardy H, Yeh S. Infertility with defective spermatogenesis and hypotestosteronemia in male mice lacking the androgen receptor in Sertoli cells. Proc Natl Acad Sci U S A 2004; 101:6876–6881.
12. De Gendt K, Swinnen JV, Saunders PT, Schoonjans L, Dewerchin M, Devos A, Tan K, Atanassova N, Claessens F, Lecureuil C, Heyns W, Carmeliet P, Guillou F, Sharpe RM, Verhoeven G. A Sertoli cell-selective knockout of the androgen receptor causes spermatogenic arrest in meiosis. Proc Natl Acad Sci U S A 2004; 101:1327–1332.
13. Kato S, Matsumoto T, Kawano H, Sato T, Takeyama K. Function of androgen receptor in gene regulations. J Steroid Biochem Mol Biol 2004; 89–90:627–633.
14. Yong EL, Loy CJ, Sim KS. Androgen receptor gene and male infertility. Hum Reprod Update 2003; 9:1–7.
15. Kato S, Sato T, Watanabe T, Takemasa S, Masuhiro Y, Ohtake F, Matsumoto T. Function of nuclear sex hormone receptors in gene regulation. Cancer Chemother Pharmacol 2005; 56:4–9.
16. MacLean HE, Warne GL, Zajac JD. Localization of functional domains in the androgen receptor. J Steroid Biochem Mol Biol 1997; 62:233–242.
17. Heinlein CA, Chang C. Androgen receptor (AR) coregulators: an overview. Endocr Rev 2002; 23(2):175–200.
18. Wang L, Hsu CL, Chang C. Androgen receptor corepressors: an overview. Prostate 2005; 63:117–130.
19. McEwan IJ. Molecular mechanisms of androgen receptor-mediated gene regulation: structure-function analysis of the AF-1 domain. Endocr Relat Cancer 2004; 11:281–293.
20. Ishitani K, Yoshida T, Kitagawa H, Ohta H, Nozawa S, Kato S. p54nrb acts as a transcriptional coactivator for activation function 1 of the human androgen receptor. Biochem Biophys Res Commun 2003; 306:660–665.
21. Ishiguro H, Uemura H, Fujinami K, Ikeda N, Ohta S, Kubota Y. 55 kDa nuclear matrix protein (nmt55) mRNA is expressed in human prostate cancer tissue and is associated with the androgen receptor. Int J Cancer 2003; 105:26–32.
22. Fox AH, Lam YW, Leung AK, Lyon CE, Andersen J, Mann M, Lamond AI. Paraspeckles: a novel nuclear domain. Curr Biol 2002; 12:13–25.
23. Shav-Tal Y, Zipori D. PSF and p54(nrb)/NonO–multi-functional nuclear proteins. FEBS Lett 2002; 531:109–114.
24. Dong X, Shylnova O, Challis JR, Lye SJ. Identification and characterization of the protein-associated splicing factor as a negative co-regulator of the progesterone receptor. J Biol Chem 2005; 280:13329–13340.
25. Mathur M, Tucker PW, Samuels HH. PSF is a novel corepressor that mediates its effect through Sin3A and the DNA binding domain of nuclear hormone receptors. Mol Cell Biol 2001; 21:2298–2311.
26. Gozani O, Patton JG, Reed R. A novel set of spliceosome-associated proteins and the essential splicing factor PSF bind stably to pre-mRNA prior to catalytic step II of the splicing reaction. EMBO J 1994; 13:3356–3367.
27. Rosonina E, Ip JY, Calarco JA, Bakowski MA, Emili A, McCracken S, Tucker P, Ingles CJ, Blencowe BJ. Role for PSF in mediating transcriptional activator-dependent stimulation of pre-mRNA processing in vivo. Mol Cell Biol 2005; 25:6734–6746.
28. Liang S, Lutz CS. p54nrb is a component of the snRNP-free U1A (SF-A) complex that promotes pre-mRNA cleavage during polyadenylation. RNA 2006; 12:111–121.
29. Zhang Z, Carmichael GG. The fate of dsRNA in the nucleus: a p54(nrb)-containing complex mediates the nuclear retention of promiscuously A-to-I edited RNAs. Cell 2001; 106:465–75.
30. Kanai Y, Dohmae N, Hirokawa N. Kinesin transports RNA: isolation and characterization of an RNA-transporting granule. Neuron 2004; 43:513–525.
31. Straub T, Grue P, Uhse A, Lisby M, Knudsen BR, Tange TO, Westergaard O, Boege F. The RNA-splicing factor PSF/p54 controls DNA-topoisomerase I activity by a direct interaction. J Biol Chem 1998; 273:26261–26264.
32. Bladen CL, Udayakumar D, Takeda Y, Dynan WS. Identification of the polypyrimidine tract binding protein-associated splicing factor p54(nrb) complex as a candidate DNA double-strand break rejoining factor. J Biol Chem 2005; 280:5205–5210.
33. Powers CA, Mathur M, Raaka BM, Ron D, Samuels HH. TLS (translocated-in-liposarcoma) is a high-affinity interactor for steroid, thyroid hormone, and retinoid receptors. Mol Endocrinol 1998; 12:4–18.
34. Iacobazzi V, Infantino V, Costanzo P, Izzo P, Palmieri F. Functional analysis of the promoter of the mitochondrial phosphate carrier human gene: identification of activator and repressor elements and their transcription factors. Biochem J 2005; 391:613–621.
35. Deloulme JC, Prichard L, Delattre O, Storm DR. The prooncoprotein EWS binds calmodulin and is phosphorylated by protein kinase C through an IQ domain. J Biol Chem 1997; 272:27369–27377.
36. Adegbola O, Pasternack GR. A pp32-retinoblastoma protein complex modulates androgen receptor-mediated transcription and associates with components of the splicing machinery. Biochem Biophys Res Commun 2005; 334:702–708.
37. Zhang WW, Zhang LX, Busch RK, Farres J, Busch H. Purification and characterization of a DNA-binding heterodimer of 52 and 100 kDa from HeLa cells. Biochem J 1993; 290:267–272.
38. Zolotukhin AS, Michalowski D, Bear J, Smulevitch SV, Traish AM, Peng R, Patton J, Shatsky IN, Felber BK. PSF acts through the human immunodeficiency virus type 1 mRNA instability elements to regulate virus expression. Mol Cell Biol 2003; 23:6618–6630.
39. Xu J, Zhong N, Wang H, Elias JE, Kim CY, Woldman I, Pifl C, Gygi SP, Geula C, Yankner BA. The Parkinson's disease-associated DJ-1 protein is a transcriptional co-activator that protects against neuronal apoptosis. Hum Mol Genet 2005; 14:1231–1241.
40. Emili A, Shales M, McCracken S, Xie W, Tucker PW, Kobayashi R,

Blencowe BJ, Ingles CJ. Splicing and transcription-associated proteins PSF and p54nrb/nonO bind to the RNA polymerase II CTD. RNA 2002; 8:1102–1111.
41. Myojin R, Kuwahara S, Yasaki T, Matsunaga T, Sakurai T, Kimura M, Uesugi S, Kurihara Y. Expression and functional significance of mouse paraspeckle protein 1 on spermatogenesis. Biol Reprod 2004; 71:926–932.
42. Fox AH, Bond CS, Lamond AI. P54nrb Forms a Heterodimer with PSP1 That Localizes to Paraspeckles in an RNA-dependent Manner. Mol Biol Cell 2005; 16:5304–5315.
43. Suzuki T, Kitamura S, Khota R, Sugihara K, Fujimoto N, Ohta S. Estrogenic and antiandrogenic activities of 17 benzophenone derivatives used as UV stabilizers and sunscreens. Toxicol Appl Pharmacol 2005; 203:9–17.
44. Novy M, Pohn R, Andorfer P, Novy-Weiland T, Galos B, Schwarzmayr L, Rotheneder H. EAPP, a novel E2F binding protein that modulates E2F-dependent transcription. Mol Biol Cell 2005; 16:2181–2190.
45. Takahashi S, Inatome R, Yamamura H, Yanagi S. Isolation and expression of a novel mitochondrial septin that interacts with CRMP/CRAM in the developing neurones. Genes Cells 2003; 8:81–93.
46. Tabuchi Y, Ohta S, Yanai N, Obinata M, Kondo T, Fuse H, Asano S. Development of the conditionally immortalized testicular Sertoli cell line TTE3 expressing Sertoli cell specific genes from mice transgenic for temperature sensitive simian virus 40 large T antigen gene. J Urol 2002; 167:1538–1545.
47. Dai T, Vera Y, Salido EC, Yen PH. Characterization of the mouse Dazap1 gene encoding an RNA-binding protein that interacts with infertility factors DAZ and DAZL. BMC Genomics 2001; 2:6.
48. Kurihara Y, Watanabe H, Kawaguchi A, Hori T, Mishiro K, Ono M, Sawada H, Uesugi S. Dynamic changes in intranuclear and subcellular localizations of mouse Prrp/DAZAP1 during spermatogenesis: the necessity of the C-terminal proline-rich region for nuclear import and localization. Arch Histol Cytol 2004; 67:325–333.
49. Sharpe RM, McKinnell C, Kivlin C, Fisher JS. Proliferation and functional maturation of Sertoli cells, and their relevance to disorders of testis function in adulthood. Reproduction 2003; 125:769–784.
50. Meissner M, Dechat T, Gerner C, Grimm R, Foisner R, Sauermann G. Differential nuclear localization and nuclear matrix association of the splicing factors PSF and PTB. J Cell Biochem 2000; 76:559–566.
51. Shav-Tal Y, Lee B, Bar-Haim S, Vandekerckhove J, Zipori D. Enhanced proteolysis of pre-mRNA splicing factors in myeloid cells. Exp Hematol 2000; 28:1029–1038.
52. Traish AM, Huang YH, Ashba J, Pronovost M, Pavao M, McAneny DB, Moreland RB. Loss of expression of a 55 kDa nuclear protein (nmt55) in estrogen receptor-negative human breast cancer. Diagn Mol Pathol 1997; 6:209–221.
53. Boonyaratanakornkit V, Melvin V, Prendergast P, Altmann M, Ronfani L, Bianchi ME, Taraseviciene L, Nordeen SK, Allegretto EA, Edwards DP. High-mobility group chromatin proteins 1 and 2 functionally interact with steroid hormone receptors to enhance their DNA binding in vitro and transcriptional activity in mammalian cells. Mol Cell Biol 1998; 18:4471–4487.
54. Jeong BC, Hong CY, Chattopadhyay S, Park JH, Gong EY, Kim HJ, Chun SY, Lee K. Androgen receptor corepressor-19 kDa (ARR19), a leucine-rich protein that represses the transcriptional activity of androgen receptor through recruitment of histone deacetylase. Mol Endocrinol 2004; 18:13–25.
55. Ozanne DM, Brady ME, Cook S, Gaughan L, Neal DE, Robson CN. Androgen receptor nuclear translocation is facilitated by the f-actin cross-linking protein filamin. Mol Endocrinol 2000; 14:1618–1626.
56. Schrantz N, da Silva Correia J, Fowler B, Ge Q, Sun Z, Bokoch GM. Mechanism of p21-activated kinase 6-mediated inhibition of androgen receptor signaling. J Biol Chem 2004; 279:1922–1931.
57. Yang YS, Yang MC, Tucker PW, Capra JD. NonO enhances the association of many DNA-binding proteins to their targets. Nucleic Acids Res 1997; 25:2284–2292.
58. Kiesler E, Miralles F, Ostlund Farrants AK, Visa N. The Hrp65 self-interaction is mediated by an evolutionarily conserved domain and is required for nuclear import of Hrp65 isoforms that lack a nuclear localization signal. J Cell Sci 2003; 116:3949–3956.
59. Iwasaki T, Chin WW, Ko L. Identification and characterization of RRM-containing coactivator activator (CoAA) as TRBP-interacting protein, and its splice variant as a coactivator modulator (CoAM). J Biol Chem 2001; 276:33375–33383.
60. Hummelke GC, Cooney AJ. Reciprocal regulation of the mouse protamine genes by the orphan nuclear receptor germ cell nuclear factor and CREMtau. Mol Reprod Dev 2004; 68:394–407.
61. Lee CH, Chinpaisal C, Wei LN. A novel nuclear receptor heterodimerization pathway mediated by orphan receptors TR2 and TR4. J Biol Chem 1998; 273:25209–25215.

Identification of prostatic-secreted proteins in mice by mass spectrometric analysis and evaluation of lobe-specific and androgen-dependent mRNA expression

Nariaki Fujimoto, Yukimi Akimoto[1], Tomoharu Suzuki[2], Shigeyuki Kitamura[2] and Shigeru Ohta[2]

Department of Developmental Biology, Research Institute for Radiation Biology and Medicine, Hiroshima University, 1-2-3 Kasumi, Minami-ku, Hiroshima 734-8553, Japan

[1]Department of Radiation Responses, Research Institute for Radiation Biology and Medicine, Hiroshima University, 1-2-3 Kasumi, Minami-ku, Hiroshima 734-8553, Japan

[2]Department of Xenobiotic Metabolism and Molecular Toxicology, Institute of Pharmaceutical Sciences, Hiroshima University School of Medicine, Kasumi 1-2-3, Minami-ku, Hiroshima 734-8551, Japan

(Requests for offprints should be addressed to N Fujimoto; Email: nfjm@hiroshima-u.ac.jp)

Abstract

Rats and guinea pigs have frequently been used to study the development of the prostate and the mechanism of androgen action, but the mouse prostate has also become an attractive model for prostate research, because an enormous range of genetically altered mice is now available. However, the secretion of proteins in the mouse prostate has not yet been thoroughly investigated. In the present study, major secreted proteins from the ventral prostate (VP), dorsolateral prostate (DLP), and anterior prostate (AP) of mice were identified by means of 2D-gel electrophoresis followed by MALDI-TOF mass spectrometric analysis. A quantitative reverse transcriptase-PCR method was further employed to examine the androgen-dependent transcriptional regulation of the identified proteins. Proteome analysis revealed that the VP secretes spermine-binding protein, serine protease inhibitor Kazal type-3, and a 91 kDa hypothetical scavenger receptor (AK035662). DLP and AP secrete a protein similar to immunoglobulin-binding protein, immunoglobulin-binding protein-like protein, and one of the experimental autoimmune prostatitis antigen proteins (EAPA2). Peroxiredoxin-6, glucose-regulated protein 78, zinc-α2-glycoprotein, and phospholipase Cα are also secreted. Castration of animals led to a decrease in the mRNAs of these secreted proteins, although the extents of changes varied greatly among different lobes. We present here an outlined view of mouse prostate secretion, which should contribute to an understanding of the biological functions of the prostate gland, as well as the androgen dependency of prostate secretion.

Journal of Endocrinology (2006) **190,** 793–803

Introduction

Rat models have been widely used to study prostate morphology, development, and pathology, as well as androgen-regulated gene expression, in order to understand the basic functions and pathology of this male accessory sex gland (Cunha *et al.* 1987). Mice have generally not been used because the small size of the gland makes morphological studies difficult, and because the mouse prostate is less susceptible to carcinogenesis (Shirai *et al.* 2000). Recently, however, a huge range of transgenic and knockout mice has become available with considerable potential for studies of the prostate (Abate-Shen & Shen 2002, Klein 2005). Transgenic adenocarcinoma of the mouse prostate (TRAMP) mice has been used to study the progression and chemoprevention of prostate cancer (Greenberg *et al.* 1995). Prolactin transgenic mice have been used to investigate the effect of prolactin on prostate growth (Wennbo *et al.* 1997). Estrogen receptor knockout mice (αERKO and βERKO) have been used to examine the role of estrogen in prostate development (Weihua *et al.* 2001, Omoto *et al.* 2005). Aromatase knockout, prolactin receptor knockout, and conditional deletion of Rb mice have been used to study the involvement of those genes in prostate carcinogenesis (McPherson *et al.* 2001, Robertson *et al.* 2003, Maddison *et al.* 2004). However, despite these recent developments, the basic biological function of the prostate, prostatic secretion, is still poorly understood in the mouse. Identification of the secreted proteins will be helpful in understanding prostate development and pathology.

The rodent prostate consists of the ventral prostate (VP), lateral prostate (LP), dorsal prostate (DP), and anterior prostate (AP or coagulating gland). It is well known that rat prostatic secretory proteins, such as prostatein and cystatin-related protein, are mainly produced in the VP, and other proteins, such as prostatic secretory protein of 94 aa (PSP94), probasin,

Journal of Endocrinology (2006) **190,** 793–803
0022–0795/06/0190–793 © 2006 Society for Endocrinology *Printed in Great Britain*
DOI: 10.1677/joe.1.06733
Online version via http://www.endocrinology-journals.org

and seminal vesicle secretion 2 (SVS2) are abundant in the LP and DP (Cunha *et al.* 1987). An early study revealed that spermine-binding protein (SBP) and serine protease inhibitor Kazal type-3 (SPI-KT3) are abundant in the mouse VP (Mills *et al.* 1987*a*, 1987*b*). Proteins secreted from the dorso-lateral prostate (DLP) and AP have not yet been identified, although Cunha's group developed a specific polyclonal antibody for major DLP protein(s) to be used as a differentiation marker (Donjacour *et al.* 1990).

In the present study, the major proteins secreted from the VP, DLP, and AP were identified by means of 2D-gel electrophoresis followed by MALDI-TOF mass spectrometric analysis. Further, a quantitative reverse transcriptase (RT)-PCR method was employed to examine the androgen dependence of the transcriptional regulation of the secretory proteins.

Materials and Methods

Animals

Animal experiments were conducted in accordance with *A Guide for the Care and Use of Laboratory Animals of Hiroshima University.* The male C57BL mice were purchased from Charles River Japan Co. (Kanagawa, Japan) and maintained with free access to basal diet and tap water. For proteome analysis, three of the 11-week-old mice were killed under ether anesthesia and the prostate and seminal vesicle (SV) were carefully dissected out. In addition, four animals were used for evaluating the sample preparation method. For the study of age-dependent mRNA expression, animals were killed at 1, 2, 4, 6, and 11 weeks (four animals per group), and each of the prostate lobes was dissected under a microscope and immediately fixed in RNA Later solution (Ambion, Inc., Austin, TX, USA). For the castration and hormone-replacement study, animals were divided into three groups, the castrated, castrated plus testosterone injected, and intact. Surgical castration was made at 10 weeks of age and animals were allowed to recover for 1 week. Testosterone propionate (Wako Junyaku KK, Osaka, Japan) was dissolved in the vehicle oil, Panacete 810 (Nippon Oils and Fats Co., Ltd, Tokyo, Japan), and the solution was administered i.p. at a dose of 5 mg/kg body weight. Animals were killed under ether anesthesia 24 h after testosterone injection, and the prostate lobes were collected for RNA extraction.

Preparation of secretion samples

Preparation of secretion samples was performed based on the previously reported method (Donjacour *et al.* 1990). Each dissected prostate lobe from an 11-week-old mouse was rinsed well in saline and placed on a 35 mm culture dish with 100 µl saline containing 1% protease inhibitor mixture (Sigma). Each lobe was cut into four or five pieces, left to stand for 5 min, and transferred to a 1·5 ml microcentrifuge tube. After centrifugation at 10 000 *g* for 5 min at room temperature, the supernatant was collected as the secretion sample. The incubation time of 5 min was chosen because inner cellular contamination (glyceraldehyde-3-phosphate dehydrogenase; GAPDH) was confirmed to below by 5 min (Fig. 1). For the SV secretion sample, the content of the vesicle was collected and suspended in saline with protease inhibitors. The protein concentration of each sample solution was determined with a Protein Assay kit (Bio-Rad Lab.). For de-glycosidation, samples were incubated with PNGase F (50 U/µg protein; New England Biolabs, Ipswich, MA, USA) at 37 °C for 1·5 h.

Electrophoresis (1D and 2D-PAGE)

For SDS-PAGE gel electrophoresis, 15 µg total protein of each sample were mixed with the SDS-PAGE buffer containing 2-mercaptoethanol, and applied to a 5–20% gradient PAGE gel (10×10 cm^2 SuperSep pre-cast gel; Wako Jyunyaku) with molecular weight markers, Precision Plus (Bio-Rad Lab.). The electrophoresis was carried out at a constant current of 20 mA. The gel was fixed and stained with 45% methanol and 10% acetic acid containing 0·2% Coomassie Brilliant Blue, followed by de-staining with 7% methanol and 7% acetic acid.

For 2D-gel electrophoresis, 1D isoelectric focusing with immobilized pH gradients was performed with Immobiline

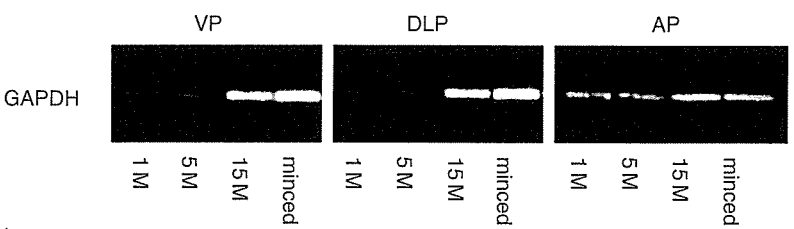

Figure 1 Intracellular contamination in secretion samples. Each prostatic lobe was cut into four or five pieces, and secretion out of the prostatic canals was allowed for 1, 5, and 15 min. Then the lobes were centrifuged and the supernatant was collected as the secretion sample. The samples were applied to the SDS-PAGE (5–20%) at 0·3 µg protein/lane, transferred to a piece of PVDF membrane and immunostained with antibody to GAPDH, an inner cellular marker (36 kDa band). The intracellular contamination was lesser in the samples incubated for 1 and 5 min (1, 5 M) than in those incubated for 15 min (15 M) or prepared from minced tissues (minced). The incubation time of 5 min was chosen for sample preparation in the present study.

DryStrip (Amersham) and the Ettan IPGphor system (Amersham) according to the manufacturer's protocol. For analytical 2D-PAGE, 10 μg de-glycosidated protein was applied in a 7 cm Immobiline DryStrip (pI 3–11, nonlinear gradient). After rehydration, the strip was isoelectrofocused (15 kVh). The Immobiline gel was then treated with SDS equilibration buffer (50 mM Tris–HCl, pH 8·8, 6 M urea, 30% glycerol, and 2% SDS) containing 10 mg/ml DTT for 15 min, followed by the same buffer containing 25 mg/ml iodoacetamide. The Immobiline gel was then placed on the second SDS-PAGE slab gel with 5–20% gradient (SuperSep pre-cast gel, Wako Jyunyaku) and overlaid with hot agarose solution to connect the two gels. The second electrophoresis was run at a constant current of 20 mA. The gel was fixed with 50% methanol and 7% acetic acid, stained overnight in Sypro Ruby (Invitrogen), and de-stained with 10% methanol and 7% acetic acid. Stained gels were scanned with a Molecular Imager FX Pro (Bio-Rad Lab.), with excitation at 532 nm. In the case of preparative 2D-PAGE for mass spectrometric analysis, 60 μg total protein were subjected to electrophoresis as described previously and then stained with silver nitrate by incubation with 0·2 g/l $Na_2S_2O_3$ for 1 min followed by 1 g/l $AgNO_3$ for 20 min on ice, and washed with 20 g/l Na_2CO_3 containing 0·1% HCHO. A 24 cm Immobiline DryStrip (pI, 3–11) was also used for preparation. It was rehydrated with 200 μg secreted protein and isoelectrofocused (25 kVh), then placed on 12·5% SDS-PAGE gel and overlaid with hot agarose solution. The electrophoresis was performed at a constant current of 400 mA. The gel was stained with silver nitrate as described earlier. Three sets of secretion samples from different animals were applied to 2D-electrophoresis and analyzed.

Western blotting

Total proteins, 0·3 μg of each preparation of prostate secretion, were applied to SDS-PAGE (5–20% gel). Proteins were then transferred to a piece of Hybond-P polyvinylidene difluoride (PVDF) membrane (Amersham). The membrane was incubated with a monoclonal antibody to GAPDH (Ambion) at 1 μg/ml followed by a peroxidase-conjugated antibody to mouse IgG (MBL Co., Nagoya, Japan) at a dilution of 1:1000. Protein bands were detected using the ECL system (Amersham).

Mass spectrometry (MS)

The protein spots were excised from the polyacrylamide gel and silver nitrate was removed with 15 mM $K_3[Fe(CN)_6]$ and 50 mM $Na_2S_2O_3$. The gel pieces were incubated in distilled water for 1 h, incubated with CH_3CN for 10 min, and dried in a centrifuge-vacuum concentration system. Each gel piece was incubated with a 20 μl aliquot of 10 μg/ml trypsin solution (sequence grade, Sigma) for 30 min on ice. Excess trypsin solution was removed, and the gel piece was incubated overnight at 35 °C. To extract the digested peptides, 10 μl of 70% CH_3CN containing 0·1% trifluoroacetic acid were added to each gel piece. An aliquot of 0·5 μl of the extract solution was spotted onto a target plate for an UltraFlex mass spectrometer (Bruker Daltonics, Bremen, Germany) along with 0·5 μl of 10 mg/ml α-cyano-4-hydroxycinnamic acid (MS grade, Nacalai tesque Co., Kyoto, Japan). MS was performed using an accelerating voltage of 20 kV, with data acquisition between 1000 and 4000 Da. Some of the fragment peaks were further analyzed by MS/MS. The MS and MS/MS data were evaluated with Biotools software (Bruker Daltonics) in combination with a peptide mass fingerprinting analysis system, MASCOT version 2·1 (Matrix Science, London, UK). The peptide mass fingerprinting was performed based on mass spectroscopy protein sequence database (MSDB; Imperial College London, UK) and the nr database at the National Centre for Biotechnology Information (NCBInr; Bethesda, MD, USA) with terminal modifications of peptides set as fixed carbamidomethyl and flexible oxidation ends. The peptide mass tolerance was set to 0·3%.

Quantification of mRNAs by real-time RT-PCR

Total RNA was prepared from each lobe of the prostate with an RNA Isolation kit (Promega), and 2 μg total RNA were reverse transcribed as described previously (Fujimoto *et al.* 2004). An ABI Prism 7700 (Perkin–Elmer Life Sciences, Boston, MA, USA) was employed for quantitative measurement of cDNA using a QuantiTect Sybr Green PCR kit (Qiagen). Specific primer sets with a T_m of about 59 °C were designed for each mRNA (Table 1). Prior to quantitative analysis, PCR products were prepared separately and purified by gel electrophoresis. The DNA sequences were confirmed with a capillary DNA sequencer, ABI 310 (Perkin–Elmer Life Sciences). Extracted fragments were used as standards for quantification. The PCR conditions were 15 min of initial activation followed by 45 cycles of 20 s at 94 °C, 30 s at 58 °C, and 40 s at 72 °C. All mRNA contents were normalized with reference to β-actin mRNA.

Serum testosterone levels

Serum testosterone levels were measured with an ELISA kit, purchased from Neogen Corp. (Lexington, KY, USA).

Statistical analysis

Statistical comparisons were made using Student's *t*-test.

Results

1D-PAGE analysis

The secretory proteins from the VP, DLP, AP, and SV were treated with a de-glycosidation enzyme, PNGase F, and analyzed with SDS-PAGE (Fig. 2). In the VP, a broad band at 20–25 kDa was evidently the major band, and a 10 kDa band

Table 1 Quantitative PCR primers for mouse genes

	GenBank accession #	5′-Primer (5′→3′)	3′-Primer (5′→3′)
Genes			
91 kDa protein	AK035662	GGACCTTCCACAAGCGAACAT	GCACTCCTCCAGGTGTTCCTC
AGR2	M_011783	TTCATCACTTGGACGAATGCC	ACGTACTGGCCATCAGGAGAA
Calr	NM_007591	ACCGTGAAGCATGAGCAGAAT	TGTTGATCAGCACATTCTTGCC
EAPA2	AY528666	CCAGACAGGCAGAATTGGGTT	CTCCTCGGAATCTATATTGGCG
GRP78	NM_022310	TCTTGCCATTCAAGGTGGTTG	TTCTTTCCCAAATACGCCTCAG
IgBPLP	XM_620455	CTGTGAGTTGCCCGAGCCT	CACAATGGAGAACGCCTCCT
PDI	MUSPDIA	CGCAACAACTTTGAGGGTGA	TTGGGCAGGAACAGCAGAAT
PLCα	M73329	ATTGCACTGCCAACACAAACA	AACTGAAGCTGGTCCTGCTTG
Prdx6	BC013489	AGGACGCTAACAACATGCCTG	GTGCCTGTCAGCTGGAGAGAG
Probasin	AF005204	ACACTGCATGTGCTAGGCGT	TCCCACACAAAATGTGACGG
PSP94	U89840	CCAACGCTACTAGGCCTTTGA	GCCCACACGAAGCACATTTAC
SBP	NM_011321	TGGAACCCGGTCAGATAACTTT	TCGACCCCTTCTAACACCAAA
SPI-KT3	BC086887	AGAGGCTAGTTGCCATGATGC	GGACAGGCTCTATGCGTTTCC
SVS2	NM_009300	CAGAGCAGCTCCTCAGAGGG	TCTGGGTCATGTCACCACCA
ZnG	AF281658	CCCACAGGACATAGACCCCTT	CTCATGTCAGGCAGAGAGGGTA
β-Actin	X03765	CTGTCCCTGTATGCCTCTGGTC	TGAGGTAGTCCGTCAGGTCCC

seemed to be secondary. PNGase F treatment shifted the major band to a sharper 19 kDa band, while other bands were unaffected. The main band in the DLP appeared to be a broad band at 80–100 kDa, together with bands at 17 and 13 kDa. PNGase F digested the major band into two sharper bands of approximately 80 and 90 kDa, which showed lower staining intensities. The mobility of other bands was not changed much by PNGase F treatment, although some smear-like

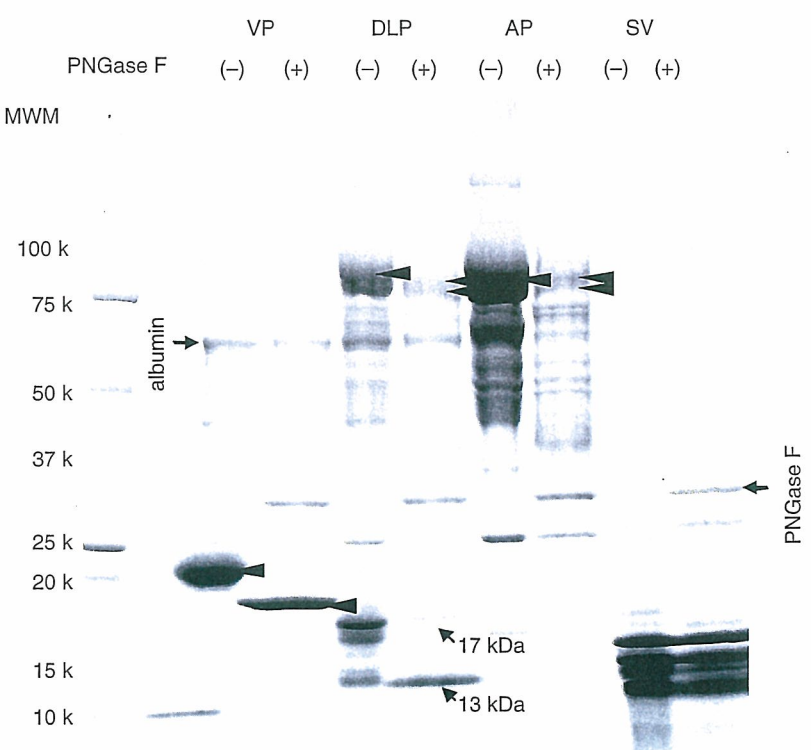

Figure 2 1D-SDS-PAGE analysis of mouse prostate secretory proteins. Secretion was prepared from the VP, DLP, and AP, as well as the SV. Each sample was incubated with (+) or without (−) PNGase F and applied to a 5–20% gradient SDS-PAGE gel. The gel was stained with Coomassie Brilliant Blue. Arrows indicate major shifted bands by PNGase.

staining disappeared. When the AP was compared with the DLP, the patterns of bands larger than 25 kDa were similar, as was the effect of PNGase digestion. However, several DLP-specific bands were present in the molecular weight range below 25 kDa. A band of albumin, 68 kDa, representing contamination from serum, was present in the preparations of prostatic secretion, especially in the VP and DLP. The pattern of SV protein bands was completely different from those of prostatic proteins. The major SV bands were observed between 10 and 16 kDa.

2D-PAGE and identified proteins

Secretory proteins from all the lobes were treated with PNGase F and subjected to 2D-PAGE analysis. Owing to the limitation in the pore size of the immobilized pH gradient gel for isoelectric focusing, proteins with a molecular mass of over 100 kDa could not be analyzed in the 2D-PAGE. Gels were stained and the major spots were picked up for MS analysis (Fig. 3). The analysis of three sets of prostate secretions from independent control mice provided identical patterns. The spots were successfully identified and the results were summarized in Table 2. SBP and SPI-KT3 were major proteins in the VP. In addition, a 91 kDa protein, predicted from urinary bladder cDNA data (AK035662) was identified in the VP, along with glucose-regulated protein 78 (GRP78 or heat-shock 70 kDa protein 5) and peroxiredoxin 6 (Prdx6). Two higher molecular weight proteins in the DLP and AP were identified as experimental autoimmune prostatitis antigen 2 (EAPA2) and a predicted protein similar to immunoglobulin-binding protein (immunoglobulin binding protein-like protein; IgBPLP). Zn-α2-glycoprotein (ZnG), a mammalian homologue of *Xenopus* anterior gradient 2 (AGR2), as well as PSP94 and probasin, were detected in the DLP secretion. Phospholipase Cα (PLCα), calreticulin (Calr), and protein disulfide isomerase were also identified in both DLP and AP secretions. SVS2, 4, 5, and 6 were identified in the SV fluid.

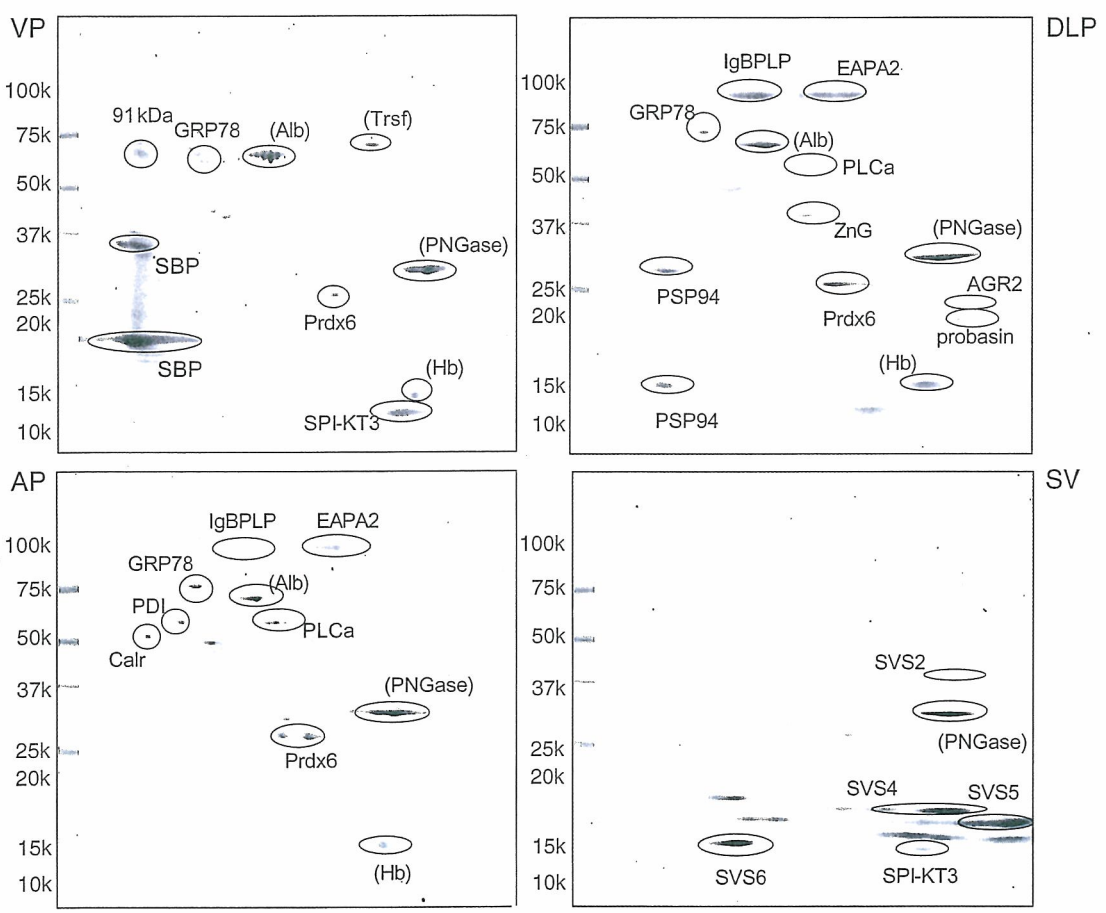

Figure 3 2D-PAGE analysis of mouse prostate secretory proteins. Each sample from the VP, DLP, AP, and SV was treated with PNGase F and applied to an immobilized pH gradient gel, followed by a second SDS-PAGE. Gels were stained with Sypro Ruby. The identified spots are indicated in the figure. Serum albumin (Alb), transferrin (Trsf), and hemoglobin (Hb) were considered to be due to serum contamination.

Table 2 Identified mouse prostatic secretory proteins

Abbreviation	Protein name	Accession #	Observed MW/pI	Theoretial MW/pI	*P*	Sequence coverage (%)
SBP	Spermine-binding protein	NP_035451	18,35/4·5	22/4·6	0·999	46
91 kDa	Protein predicted from cDNA AK035662	Q8BZE1	80/4·5	93/4·8	0·973	13
GRP78	Glucose-regulated protein 78 kDa	A37048	70/5·0	72/5·0	1·000	39
Prdx6	Peroxiredoxin 6	O08709	25/6·0, 6·5	25/5·6	1·000	57
SPI-KT3	Serine protease inhibitor, KT3	NP_033284	10/7·5	9/8·0	1·000	40
PSP94	Prostatic-secretory protein 94	NP_065622	13,28/5·0	13/5·5	1·000	76
IgBPLP	IgG-binding protein-like protein	XP_620455	100/ 5·5	210/5·5	1·000	28
EAPA2	Experimental auto-immune prostatitis antigen 2	NP_98193	100/6·5	103/6·2	1·000	42
PLCα	Phospholipase Cα	AAA39944	55/6·0	57/6·0	1·000	29
ZnG	Zinc-α2-glyco-protein	Q64726	35/6·0	34/5·8	0·992	28
AGR2	Homolog of *Xenopus* anterior gradient 2	BAB25181	20/9·5	20/9·5	1·000	56
Probasin	Probasin	AAC01954	22/9·5	21/10·1	1·000	56
Calr	Calreticulin	NP_031617	50/4·5	48/4·2	1·000	35
PDI	Protein disulfide isomerase	AAA39906	60/5·0	57/4·6	0·972	35

Lobe-specific mRNA expression of identified secreted proteins

Expression of identified proteins in the prostate was further confirmed by examining the mRNA levels; the results are summarized in Table 3. Lobe-specific expression of secreted proteins was evident. Both SBP and SPI-KT3 mRNAs were extremely abundant in the VP but virtually undetectable in the other lobes. The mRNA expression of the 91 kDa protein was also VP-specific. Abundant expression of IgGBPLP and EAPA2 mRNA was detected in the DLP and AP. Probasin expression was specific to the DLP/AP, while PSP94 mRNA was specific to the VP/DLP. The level of ZnG mRNA was highest in the DLP. The other protein mRNAs were expressed uniformly among the prostatic lobes.

Androgen dependency in mRNA expression of identified secreted proteins

Transcriptional regulation of identified proteins by androgen was examined by comparing mRNA levels among castrated, castrated plus testosterone-treated, and intact animals (Table 4). Serum

Table 3 mRNA levels of identified proteins in each prostatic lobe in 11-week-old mice

	SBP	SPIKT3	91 kDa	PSP94	ZnG	GRP78	AGR2
VP	511±58·9	184±36·0	3·6±0·8	2·6±0·6	0·9±0·1	1·7±0·5	0·14±0·03
DLP	0	0	0	5·8±1·5	12·3±1·1	6·1±1·7	0·38±0·04
AP	0	0	0	0	1·4±0·3	2·7±0·2	0·54±0·04
	PLCa	**Calr**	**PDI**	**Prdx6**	**Probasin**	**EAPA2**	**IgBPLP**
VP	0·17±0·021	0·7±0·1	15·0±2·1	2·5±0·3	0·06±0·02	0	0·0±0·0
DLP	0·36±0·085	1·2±0·3	8·3±2·1	21·7±2·6	2·15±0·23	18·9±1·5	67·9±10·3
AP	0·60±0·088	1·1±0·3	4·0±0·8	29·0±5·6	0·78±0·05	5·5±0·8	53·0±0·3

Means±S.E.M. (n=5). Values are mRNA levels divided by β-actin mRNA levels (mol/mol β-actin). 11-week-old male C57BL mice were killed and total RNA was isolated from each prostate lobe. mRNA levels were measured by real-time RT-PCR.

Table 4 Androgen regulation of mRNA levels of identified proteins

	SBP	SPIKT3	91 kDa	PSP94	ZnG	GRP78	AGR2
VP							
Cast	8·2±0·91[a]	0·24±0·08	0·09±0·02	0·011±0·004	0·38±0·032	0·57±0·36	0·03±0·004
Cast+T	48±7·9 (5·9)[b]	9·3±3·2 (39)	0·8±0·23 (8·4)	0·4±0·008 (38)	0·56±0·10 (1·5)	1·02±0·14 (1·8)	0·14±0·03 (4·9)
Intact	511±58·9 (62)	184±36 (769)	3·6±0·79 (40)	2·6±0·55 (236)	0·92±0·09 (2·4)	1·7±0·47 (3·0)	0·12±0·02 (4·3)
DLP							
Cast	–	–	–	0·002±0·001	0·64±0·11	0·55±0·11	0·01±0·001
Cast+T	–	–	–	0·08±0·046 (38)	2·0±0·48 (3·1)	3·4±0·73 (1·8)	0·06±0·02 (6·9)
Intact	–	–	–	5·8±1·48 (2633)	12·3±1·1 (19)	6·1±1·7 (11)	0·38±0·04 (45)
AP							
Cast	–	–	–	–	0·06±0·01	0·33±0·59	0·01±0·002
Cast+T	–	–	–	–	0·21±0·05 (3·6)	1·33±0·19 (4·1)	0·08±0·013 (9·5)
Intact	–	–	–	–	1·4±0·3 (24)	2·7±0·22 (8·3)	0·54±0·04 (64)

	PLCa	Calr	PDI	Prdx6	Probasin	EAPA2	IgBPLP
VP							
Cast	0·14±0·081	0·2±0·03	5·6±1·2	3·7±0·73	–	–	–
Cast+T	0·23±0·03 (1·6)	0·7+0·1 (3·3)	11·7±2·1 (2·1)	3·8±1·41 (1·0)	–	–	–
Intact	0·17±0·021 (1·2)	0·7+0·09 (3·5)	15·0±2·1 (2·7)	2·5±0·3 (0·7)	–	–	–
DLP							
Cast	0·09±0·014	0·2±0·05	1·7±0·32	1·5±0·41	0·02±0·003	0·19±0·072	1·2±0·29
Cast+T	0·15±0·02 (1·7)	0·3+0·07 (1·5)	4·5±1·0 (2·7)	2·1±0·22 (1·4)	0·05±0·002 (2·3)	2·4±0·55 (13)	1·6±0·6 (1·4)
Intact	0·36±0·085 (4·0)	1·2+0·3 (6·4)	8·3±2·1 (5·0)	21·7±2·6 (14)	2·2±0·23 (124)	18·9±1·5 (102)	67·9±10·3 (58)
AP							
Cast	0·20±0·03	0·4±0·06	1·4±0·3	1·2±0·15	0·02±0·004	0·17±0·52	0·25±0·18
Cast+T	0·34±0·085 (1·7)	0·7±0·05 (1·8)	2·8±0·5 (2·0)	4·7±0·93 (4·0)	0·04±0·008 (2·6)	4·8±0·9 (29)	1·1±0·8 (4·4)
Intact	0·60±0·088 (3·0)	1·1±0·3 (2·8)	4·0±0·8 (2·8)	29·0±5·6 (25)	0·78±0·051 (49)	5·5±0·8 (33)	53·0±0·31 (215)

[a]Mean±S.E.M. (n=5). Values are mRNA levels divided by β-actin mRNA levels (mol/mol β-actin).
[b]Values in parenthesis are fold change in mRNA over the castrated.10-week-old male C57BL mice were castrated and maintained for a week (cast). They were killed 24 h after testosterone administration at 5 mg/kg bw, ip (Cast+T). Total RNA was isolated from each prostate lobe and amounts of mRNA were measured by real-time RT-PCR.